

## Particle-Hole States in the Alpha Particle with Realistic Forces\*

B. R. BARRETT†

*Institute of Theoretical Physics, Department of Physics, Stanford University, Stanford, California*

(Received 6 June 1966)

We solve the Tamm-Dancoff equations, using the realistic separable potential of Tabakin, for the odd-parity excited states of  ${}^4\text{He}$ . A comparison is made with results obtained using the hard-core potentials of Brueckner, Gammel, and Thaler and of Hamada. The calculated spectrum is found to be strongly influenced by the  $p$ -state contributions, particularly by the effect of the tensor interaction. We predict that the  $0^-$ ,  $T=0$  state lies close to the  $2^-$ ,  $T=0$  state. The spin-orbit splitting between the  $p_{1/2}$  and  $p_{3/2}$  single-particle states is calculated and found in first order to depend only on the relative two-body spin-orbit interaction. Our estimate for the ratio of the probability of an  $E1$  transition from the upper  $1^-$ ,  $T=1$  state to the ground state to that of an  $E1$  transition from the lower  $1^-$ ,  $T=1$  state is calculated to be 1.6, compared with the experimental ratio which is  $\sim \frac{1}{2}$ . We also calculate the squared matrix elements and the total capture rate for muon capture in  ${}^4\text{He}$ . The squared matrix elements are found to be equal within 10 percent, but the calculated total capture rate is smaller than the experimental rate. Our theoretical results tend to justify the use of the supermultiplet theory for the excited states of the  $\alpha$  particle. We find that our seven equations for the energy splittings depend upon only four quantities. Consequently, we are able to obtain three relations, which give the two unobserved energy splittings and the ratio of the  $E1$  transition probabilities in terms of the four observed energy splittings. The two empirical results which can be compared with experiment are in excellent agreement.

### I. INTRODUCTION

THE form of the interaction between nucleons inside a nucleus remains one of the most fascinating problems in nuclear physics. The work of Brueckner and Gammel<sup>1</sup> and Bethe and Goldstone<sup>2</sup> on the properties of nuclear matter showed that only the two-particle correlations are important and that one can get good results in nuclear many-body calculations using the free nucleon-nucleon interaction. This result encouraged physicists to try calculations for finite nuclei using realistic two-nucleon potentials. The application of the Brueckner theory or the "independent pair model" to finite nuclei was carried out by Brueckner *et al.*<sup>3,4</sup> and by Eden and his co-workers,<sup>5-7</sup> who calculated the binding energy and density of  ${}^{16}\text{O}$ .

Ideally one would like to perform a completely self-consistent shell-model calculation for finite nuclei in which the effective interaction between nucleons is taken to be the free nucleon-nucleon interaction. Such a calculation would involve, first of all, doing a Hartree-Fock (H-F) calculation using the free nucleon-nucleon potential in order to determine the shell-model single-particle (S-P) energies and wave functions. One could then do a shell-model calculation of the spectra of finite

nuclei using these S-P energies and wave functions and again taking the free nucleon-nucleon potential as the effective interaction between nucleons. However, the singular nature of the hard-core nuclear potential has prevented physicists from doing the H-F calculation. New nonsingular and nonlocal forms of the free nucleon-nucleon potential have now made such a H-F calculation possible, and it has been carried out by Marthukrishnan and Baranger<sup>8</sup> using a nonlocal separable potential, by Kerman *et al.*<sup>9</sup> using the separable potential of Tabakin,<sup>10</sup> and by Davies *et al.*<sup>11</sup> using a nonlocal velocity-dependent interaction. All of them obtain fairly good agreement with the experimental S-P energies, but they also agree that their results need to be improved and that the potentials which they used need to be refined or better determined. So far no one has tried to use the results of any of these calculations to do a shell-model calculation of the spectra of finite nuclei.

Since nuclear H-F calculations could not be carried out until recently, shell-model calculations were performed by taking the S-P energies as parameters or as given by the experimental S-P levels in neighboring nuclei and by choosing harmonic-oscillator wave functions as the S-P wave functions. These choices were assumed to be good approximations for the actual S-P energies and wave functions in finite nuclei. Actually the S-P wave functions are better approximated by Woods-Saxon wave functions, but they are difficult to use in making calculations.

<sup>8</sup> R. Muthukrishnan and M. Baranger, Phys. Letters **18**, 160 (1965).

<sup>9</sup> A. K. Kerman, J. P. Svenne, and F. M. H. Villars, Phys. Rev. **147**, 710 (1966).

<sup>10</sup> F. Tabakin, Ann. Phys. (N. Y.) **30**, 51 (1964). We also want to thank Professor F. Tabakin for a private communication regarding the parameters of his potential.

<sup>11</sup> K. T. R. Davies, S. J. Krieger, and M. Baranger, Nucl. Phys. **84**, 545 (1966).

\* Supported in part by the U. S. Air Force through Air Force Office of Scientific Research Contract No. AF49(638)-1389.

† National Science Foundation Predoctoral Fellow.

<sup>1</sup> K. A. Brueckner and J. L. Gammel, Phys. Rev. **109**, 1023 (1958). See this paper for other references.

<sup>2</sup> H. Bethe and J. Goldstone, Proc. Roy. Soc. (London) **A238**, 551 (1957).

<sup>3</sup> K. A. Brueckner, J. L. Gammel, and H. Weitzner, Phys. Rev. **110**, 431 (1958).

<sup>4</sup> K. A. Brueckner, A. M. Lockett, and M. Rotenberg, Phys. Rev. **121**, 255 (1961).

<sup>5</sup> R. J. Eden, Proc. Roy. Soc. (London) **A235**, 408 (1956).

<sup>6</sup> R. J. Eden and V. J. Emery, Proc. Roy. Soc. (London) **A248**, 266 (1958).

<sup>7</sup> R. J. Eden, V. J. Emery, and S. Sampanthar, Proc. Roy. Soc. (London) **A253**, 177, 186 (1959).

Having determined the S-P energies and wave functions in the above manner, physicists carried out shell-model calculations of nuclear spectra for various forms of the particle-particle interaction between nucleons.<sup>12,13</sup> One of the earliest shell-model calculations with realistic nuclear forces was performed by Dawson, Talmi, and Walecka (DTW),<sup>14</sup> who solved a Bethe-Goldstone equation, using the free nucleon-nucleon potential of Brueckner, Gammel, and Thaler (BGT),<sup>4</sup> to determine the spectrum of <sup>18</sup>O. A similar calculation for nuclei with  $A=6$  was done by Dawson and Walecka.<sup>15</sup> Recently Kuo *et al.*<sup>16</sup> carried out a shell-model calculation of the low-lying states of the tin isotopes using the Tabakin potential. Their results were in very good agreement with a similar calculation for the tin isotopes performed by Kuo and Brown<sup>17</sup> using the Hamada-Johnston potential.<sup>18</sup>

In order to include the collective nature of nuclear states, physicists have used the theory of particle-hole states to calculate nuclear spectra. The theory of particle-hole states in closed-shell nuclei was discussed by Thouless<sup>19</sup> in an extensive article on the applications of Green's functions in low-energy nuclear physics. The theory can also be developed in terms of the "linearization method," as described by Lane.<sup>20</sup> One would like to relate the particle-hole interactions in finite nuclei to the particle-particle interactions in a manner similar to that used by Galitskii<sup>21</sup> in the nonideal Fermi gas and then to treat the particle-particle interaction in terms of a Bethe-Salpeter equation. Such a calculation is very difficult and so far has not been performed. We plan to work on this problem in the future, but restrict ourselves at the present time to the theory of particle-hole interactions in lowest order, which is equivalent to the Tamm-Dancoff (TD) or the random-phase approximation (RPA), depending upon which states are kept in the calculation.<sup>20</sup> Employing the separation method of Scott and Moszkowski<sup>22</sup> to get around the problem of the infinite hard core, Kallio and Kolltveit<sup>23</sup> and Green *et al.*<sup>24</sup> have calculated the spectrum of the odd-parity

excited states of <sup>16</sup>O using a realistic two-nucleon force in both the TD and RPA.

Within the last few months de-Shalit and Walecka (SW)<sup>25</sup> have formulated the particle-hole theory of the  $\alpha$  particle in the TD approximation and solved the resulting equations for the seven negative-parity excited states of <sup>4</sup>He. To simplify calculations they assumed a Serber force for the particle-particle interaction. Since they had ruled out  $p$ -state interactions by their choice of the nuclear force, they had to include the spin-orbit splitting as an empirical parameter in their calculation, which, in turn, led to the Landé interval rule for the ordering of the  $J^-, T=0$  states. After making these assumptions, their calculated spectrum was in excellent agreement with the five odd-parity states which have so far been observed for nuclei with  $A=4$ . However, their calculated value for the ratio of the  $E1$  transition probability of the upper  $1^-, T=1$  state to the ground state with respect to that of the lower  $1^-, T=1$  state was much larger than the observed ratio.

In this paper we plan to repeat the calculation of SW but this time using realistic nucleon-nucleon potentials. We want to see how close we can get to the experimental spectrum for a *no-adjustable-parameter* calculation and to observe what new physical predictions can be made from the use of realistic forces in this calculation. First we shall perform the calculation in first and second order using the separable potential of Tabakin, which eliminates the problem of the singular hard core. Then for comparison we shall repeat the calculation in first order for several other realistic nuclear potentials, including the singular, hard-core potentials of BGT<sup>4</sup> and Hamada<sup>26</sup> and the separable potential of Mitra *et al.*<sup>27</sup>

The  $\alpha$  particle deserves further study for several reasons:

(i) Among the light nuclei <sup>4</sup>He has the highest symmetry and is a simple system with which to make calculations. As SW have already pointed out, the negative-parity excited states of the  $\alpha$  particle make up a 15-dimensional  $SU(4)$  supermultiplet and the splittings within the supermultiplet are caused by the spin-dependent parts of the nucleon-nucleon interaction. Thus, by performing our calculations with realistic nuclear potentials, which contain tensor and spin-orbit parts as well as triplet and singlet parts, we shall be able to determine to what extent the supermultiplet is split by the different spin-dependent forces. In turn, the magnitude of these splittings will give us a check on the validity of the supermultiplet theory which assumes that the intrinsic splittings are small relative to the excitation of the center of gravity of the supermultiplet caused by the spin-independent forces.

<sup>12</sup> J. P. Elliott and B. H. Flowers, Proc. Roy. Soc. (London) **A229**, 536 (1955).

<sup>13</sup> W. W. True and K. W. Ford, Phys. Rev. **109**, 1675 (1958).

<sup>14</sup> J. F. Dawson, I. Talmi, and J. D. Walecka, Ann. Phys. (N. Y.) **18**, 339 (1962).

<sup>15</sup> J. F. Dawson and J. D. Walecka, Ann. Phys. (N. Y.) **22**, 133 (1963).

<sup>16</sup> T. T. S. Kuo, E. Baranger, and M. Baranger, Nucl. Phys. **81**, 241 (1966).

<sup>17</sup> T. T. S. Kuo and G. E. Brown (to be published).

<sup>18</sup> T. Hamada and I. D. Johnston, Nucl. Phys. **34**, 142 (1965).

<sup>19</sup> D. J. Thouless, Rept. Progr. Phys. **27**, 53 (1964).

<sup>20</sup> A. M. Lane, *Nuclear Theory* (W. A. Benjamin, Inc., New York, 1964), Part II, p. 77.

<sup>21</sup> V. Galitskii, Zh. Eksperim. i Teor. Fiz. **34**, 151 (1958) [English transl.: Soviet Phys.—JETP **7**, 104 (1958)].

<sup>22</sup> S. A. Moszkowski and B. L. Scott, Ann. Phys. (N. Y.) **11**, 65 (1960).

<sup>23</sup> A. Kallio and K. Kolltveit, Nucl. Phys. **53**, 87 (1964).

<sup>24</sup> A. M. Green, A. Kallio, and K. Kolltveit, Phys. Letters **14**, 142 (1965).

<sup>25</sup> A. de-Shalit and J. D. Walecka, Phys. Rev. **147**, 763 (1966).

<sup>26</sup> T. Hamada, Progr. Theoret. Phys. (Kyoto) **24**, 1033 (1960); **25**, 247 (1960).

<sup>27</sup> A. N. Mitra and J. H. Naqvi, Nucl. Phys. **25**, 307 (1961). See this paper for other references.

(ii) In the future we plan to carry out similar calculations for bigger nuclei, such as  $^{12}\text{C}$  and  $^{16}\text{O}$ . Thus, by performing a calculation for a very light nucleus, like  $^4\text{He}$ , we get some idea of the kind of results we can expect from a calculation such as ours. In turn, future calculations with heavier nuclei should give even better results, since our calculative assumptions, such as using harmonic-oscillator, bound-state wave functions for the excited states, should improve for bigger systems.

(iii) The  $\alpha$  particle contains some very interesting physics which has not yet been explained:

As we stated earlier, SW obtained a value for the ratio of the  $E1$  transition probability of the upper  $1^-$ ,  $T=1$  state with respect to that of the lower  $1^-$ ,  $T=1$  state that was much larger than the experimental ratio. In fact, their result predicted that most of the  $E1$  strength was in the upper  $1^-$ ,  $T=1$  state, implying  $L$ - $S$  coupling for the  $1^-$  states, while the experimental result indicates that the lower  $1^-$ ,  $T=1$  state has more  $E1$  strength than the upper state, implying  $j$ - $j$  coupling for the  $1^-$  states.

There are also unanswered questions regarding muon capture in  $^4\text{He}$ . According to the work of Foldy and Walecka (FW),<sup>28</sup> the dominant terms for muon capture in the  $\alpha$  particle come from the  $T=1$  states of the supermultiplet. Their calculations are based on the supermultiplet theory, which predicts that the squared matrix elements for muon capture are equal, i.e.,  $M_V^2 = M_A^2 = M_P^2$ , and give a value of the total muon capture rate which is smaller than and in poor agreement with the observed capture rate.

From our calculation of the  $^4\text{He}$  spectrum with realistic forces, we shall be able to determine both the ratio of the  $E1$  transition probabilities and the total muon capture rate and at the same time check the validity of the supermultiplet theory regarding the equality of the squared matrix elements.

In Sec. II we formulate our calculation, which is carried out in Sec. III. Our numerical results are also given in III, and these results are discussed and conclusions are drawn in Sec. IV.

## II. FORMULATION OF THE CALCULATION

We use the particle-hole formalism of SW for making calculations with regard to  $^4\text{He}$  in this paper, except that we compute the Talmi integrals with realistic potentials, as DTW did. We work in the shell model, using harmonic-oscillator wave functions for doing calculations, and derive the TD equations for  $^4\text{He}$  using particle-hole creation operators. In the  $j$ - $j$  coupling scheme these equations are given by<sup>25</sup>

$$\sum_{j'} \{ [(\epsilon_{p_j} - \epsilon_{s_{1/2}}) - \epsilon^{JT}] \delta_{jj'} + V_{jj'}^{JT} \} \alpha_{j'}^{JT} = 0, \quad (1)$$

where  $\epsilon_{p_j}$  and  $\epsilon_{s_{1/2}}$  are the S-P and single-hole energies, respectively,  $\epsilon^{JT}$  is the energy of the excited state with

<sup>28</sup> L. L. Foldy and J. D. Walecka, Nuovo Cimento 34, 1026 (1964).

angular momentum  $J$  and isospin  $T$ , and  $V_{jj'}^{JT}$  is the particle-hole interaction, defined by

$$V_{jj'}^{JT} = - \sum_{J'T'} (2J'+1)(2T'+1) \begin{Bmatrix} \frac{1}{2} & j' & J \\ \frac{1}{2} & j & J' \end{Bmatrix} \begin{Bmatrix} \frac{1}{2} & \frac{1}{2} & T \\ \frac{1}{2} & \frac{1}{2} & T' \end{Bmatrix} \\ \times [ \langle p_{j's_{1/2}J'T'} | V | p_{js_{1/2}J'T'} \rangle_0 - (-1)^{1/2+J+J'} \\ \times (-1)^{1/2+1/2+T'} \langle p_{j's_{1/2}J'T'} | V | s_{1/2}p_{jJ'T'} \rangle_0 ]. \quad (2)$$

The subscript 0 indicates that the expectation value is to be taken with respect to eigenstates of the unperturbed Hamiltonian,

$$H_0 = \sum_i [T(i) + \frac{1}{2} M \omega_0^2 x_i^2]. \quad (3)$$

In Eq. (3)  $\omega_0$  is the oscillator strength for  $^4\text{He}$  determined from the Coulomb energy or the electron-scattering form factor. In our calculations we use  $\omega_0$  determined by the latter method, so that

$$\hbar\omega_0 = 21.8 \text{ MeV}, \quad (4)$$

in which case the oscillator parameter  $b_0$  is given by

$$b_0 = (\hbar/M\omega_0)^{1/2} = 1.38 \text{ F}. \quad (5)$$

Similarly to SW, we now include the H-F energy of the  $p_j$  particle, i.e.,

$$V^{\text{H-F}}(p_j) = \sum_{J'T'} \frac{(2J'+1)(2T'+1)}{(2j+1)2} \\ [ \langle p_{j's_{1/2}J'T'} | V | p_{js_{1/2}J'T'} \rangle_0 - (-1)^{j+1/2-J'} \\ \times (-1)^{1/2+1/2-T'} \langle p_{j's_{1/2}J'T'} | V | s_{1/2}p_{jJ'T'} \rangle_0 ], \quad (6)$$

in the interaction matrix  $V_{jj'}^{JT}$  instead of in the configuration energy, and obtain the particle-hole energies

$$E(jJ^{\pi}T) = \frac{3}{4} \sum_{T'} (2T'+1) \begin{Bmatrix} \frac{1}{2} & \frac{1}{2} & 1 \\ T' & T & \frac{1}{2} \end{Bmatrix}^2 v_{jj}(JT') \\ + \sum_{J'} (2J'+1) \begin{Bmatrix} \frac{1}{2} & \frac{1}{2} & 1 \\ J' & J & j \end{Bmatrix}^2 v_{jj}(J'T), \quad (7)$$

where  $v_{jj}(J'T')$  is the particle-particle matrix element enclosed within the square brackets in Eq. (2). It is apparent that the off-diagonal matrix elements,  $V_{jj'}^{JT}$  ( $j \neq j'$ ), are unaffected. The coefficients

$$-(2J'+1) \begin{Bmatrix} \frac{1}{2} & j' & J \\ \frac{1}{2} & j & J' \end{Bmatrix} \begin{Bmatrix} \frac{1}{2} & \frac{1}{2} & T \\ \frac{1}{2} & \frac{1}{2} & T' \end{Bmatrix}, \\ (\frac{3}{4})(2T'+1) \begin{Bmatrix} \frac{1}{2} & \frac{1}{2} & 1 \\ T' & T & \frac{1}{2} \end{Bmatrix}^2,$$

and

$$(2J'+1) \begin{Bmatrix} \frac{1}{2} & \frac{1}{2} & 1 \\ J' & J & j \end{Bmatrix}^2$$

are tabulated in SW.

TABLE I. Contributing values of  $\mathfrak{S}$  in Eq. (9). Also shown is the relation of  $\mathfrak{S}$  to  $J$  (the total angular momentum), where  $\mathfrak{S}=\mathbf{I}+\mathbf{S}$  and  $\mathbf{J}=\mathfrak{S}+\mathfrak{L}$ .

$\mathfrak{L}$	$l$	$S$	$\mathfrak{S}$	$J$
1	0	0	0	1
0	1	0	1	1
1	0	1	1	0,1,2
0	1	1	$J$	0,1,2

We can express the particle-particle matrix elements in terms of matrix elements of the relative two-body interaction by first using a 9- $j$  symbol to go from  $j$ - $j$  to  $L$ - $S$  coupling. We then use the transformation brackets of Brody and Moshinsky<sup>29</sup> to go to relative and center-of-mass coordinates. Next we couple the relative angular momentum  $\mathbf{I}$  to the total spin  $\mathbf{S}$ , to obtain states of angular momentum,  $\mathfrak{S}$ , where  $\mathfrak{S}$  is the total angular

momentum of the two particles in the center-of-mass system. Doing this gives us two 6- $j$  symbols and a sum over allowed values of  $\mathfrak{S}$ . Thus we have the following relationships:

$$\begin{aligned}\mathfrak{S} &= \mathbf{I} + \mathbf{S}, \\ \mathbf{L} &= \mathfrak{L} + \mathbf{I} = \mathbf{I}_p + \mathbf{I}_s, \\ \mathbf{J} &= \mathfrak{S} + \mathfrak{L} = \mathbf{L} + \mathbf{S},\end{aligned}\quad (8)$$

where  $\mathbf{J}$  is the total angular momentum of the state,  $\mathbf{I}_p$  and  $\mathbf{I}_s$  are the S-P angular momenta, and  $\mathfrak{L}$  is the center-of-mass angular momentum. This procedure is similar to the one used by Kuo *et al.*<sup>16</sup> to express their particle-particle matrix elements, except that we are applying it to the particular combination of particle-particle matrix elements which is summed to give the particle-hole energies. Proceeding in the manner described above, we obtain<sup>30</sup>

$$\begin{aligned}v_{jj'}(J'T') &= \langle p_{j',s_{1/2}} J'T' | V | p_{j,s_{1/2}} J'T' \rangle_0 - (-1)^{1/2+j+J'} (-1)^{1/2+1/2+T'} \langle p_{j',s_{1/2}} J'T' | V | s_{1/2} p_j J'T' \rangle_0 \\ &= 6[(2j+1)(2j'+1)]^{1/2} \sum_{S=0}^1 (2S+1) \left\{ \begin{matrix} \frac{1}{2} & \frac{1}{2} & S \\ 1 & 0 & 1 \\ j & \frac{1}{2} & J' \end{matrix} \right\} \left\{ \begin{matrix} \frac{1}{2} & \frac{1}{2} & S \\ 1 & 0 & 1 \\ j' & \frac{1}{2} & J' \end{matrix} \right\} \sum_{\substack{l, \mathfrak{L}=0 \\ l \neq \mathfrak{L}}}^1 |\langle n=0L N=0\mathfrak{L} 1 | 01001 \rangle|^2 \\ &\quad \times \sum_{\mathfrak{S}} (2\mathfrak{S}+1) 3 \left\{ \begin{matrix} \mathfrak{L} & l & 1 \\ S & J' & \mathfrak{S} \end{matrix} \right\}^2 [1 - (-1)^{S+T'+l}] \langle (n=0LS) \mathfrak{S}T' | V | (n=0LS) \mathfrak{S}T' \rangle_0, \quad (9)\end{aligned}$$

where  $\langle 010\mathfrak{L}1 | 01001 \rangle$  is the appropriate transformation bracket for each value of  $l$  and  $\mathfrak{L}$ , and  $n$  and  $N$  are the radial quantum numbers for the relative and center-of-mass states, respectively.

We define

$$\langle (0LS) \mathfrak{S}T' | V | (0LS) \mathfrak{S}T' \rangle_0 \equiv {}^S I_l(\mathfrak{S}). \quad (10)$$

For the alpha particle, only one value of  $\mathfrak{S}$  occurs in each sum over  $\mathfrak{S}$  in Eq. (9), as indicated in Table I. From Eq. (9) we find that the *particle-particle* matrix elements are (in this notation  $S=3$  denotes the triplet spin state and  $S=1$  denotes the singlet spin state)

$$\begin{aligned}v_{1/2 \ 1/2}(0-0) &= {}^3 I_0(1), \\ v_{1/2 \ 1/2}(0-1) &= {}^3 I_1(0), \\ v_{1/2 \ 1/2}(1-0) &= \frac{1}{3} {}^1 I_1(1) + \frac{2}{3} {}^3 I_0(1), \\ v_{1/2 \ 1/2}(1-1) &= \frac{1}{3} {}^1 I_0(0) + \frac{2}{3} {}^3 I_1(1), \\ v_{3/2 \ 3/2}(1-0) &= \frac{1}{3} {}^3 I_0(1) + \frac{2}{3} {}^1 I_1(1), \\ v_{3/2 \ 3/2}(1-1) &= \frac{1}{3} {}^3 I_1(1) + \frac{2}{3} {}^1 I_0(0), \\ v_{3/2 \ 3/2}(2-0) &= {}^3 I_0(1), \\ v_{3/2 \ 3/2}(2-1) &= {}^3 I_1(2), \\ v_{1/2 \ 3/2}(1-0) &= v_{3/2 \ 1/2}(1-0) = -\frac{1}{3} \sqrt{2} [{}^3 I_0(1) - {}^1 I_1(1)], \\ v_{1/2 \ 3/2}(1-1) &= v_{3/2 \ 1/2}(1-1) = \frac{1}{3} \sqrt{2} [{}^1 I_0(0) - {}^3 I_1(1)]. \quad (11)\end{aligned}$$

Using the coefficients in Table IV of SW, we easily ob-

tain the particle-hole energies:

$$\begin{aligned}E_{1/2}(0-0) &= \frac{1}{2} [{}^1 I_1(1) + 2 {}^3 I_0(1) + 3 {}^3 I_1(0)], \\ E_{1/2}(1-0) &= \frac{1}{6} [7 {}^3 I_0(1) + 2 {}^1 I_1(1) + 6 {}^3 I_1(1) + 3 {}^1 I_0(0)], \\ E_{1/2}(0-1) &= \frac{1}{2} [{}^3 I_0(1) + 2 {}^3 I_1(0) + {}^1 I_0(0) + 2 {}^3 I_1(1)], \\ E_{1/2}(1-1) &= \frac{1}{6} [{}^1 I_1(1) + 2 {}^3 I_0(1) \\ &\quad + 3 {}^3 I_1(0) + 4 {}^1 I_0(0) + 8 {}^3 I_1(1)], \\ E_{3/2}(1-0) &= \frac{1}{6} [{}^1 I_1(1) + 8 {}^3 I_0(1) + 6 {}^1 I_0(0) + 3 {}^3 I_1(1)], \\ E_{3/2}(2-0) &= \frac{1}{2} [{}^1 I_1(1) + 2 {}^3 I_0(1) + 3 {}^3 I_1(2)], \\ E_{3/2}(1-1) &= \frac{1}{12} [4 {}^1 I_1(1) + 2 {}^3 I_0(1) + 10 {}^1 I_0(0) \\ &\quad + 5 {}^3 I_1(1) + 15 {}^3 I_1(2)], \\ E_{3/2}(2-1) &= \frac{1}{4} [2 {}^3 I_0(1) + 2 {}^1 I_0(0) + {}^3 I_1(1) + 7 {}^3 I_1(2)], \\ V_{1/2 \ 3/2}(1-0) &= V_{3/2 \ 1/2}(1-0) \\ &= \frac{1}{6} \sqrt{2} [{}^3 I_0(1) - {}^1 I_1(1) + 3 {}^1 I_0(0) - 3 {}^3 I_1(1)], \\ V_{1/2 \ 3/2}(1-1) &= V_{3/2 \ 1/2}(1-1) \\ &= \frac{1}{6} \sqrt{2} [{}^1 I_1(1) - {}^3 I_0(1) + {}^1 I_0(0) - {}^3 I_1(1)]. \quad (12)\end{aligned}$$

SW correctly treated the center-of-mass motion and showed that the state  ${}^1 P_1$ ,  $T=0$  corresponded to the spurious center-of-mass excitation. Therefore, the only  $T=0$  states of  ${}^4\text{He}$  are  ${}^3 P_{0,1,2}$ , and we can pick out the correct combination for the  $1^-$ ,  $T=0$  state by using

$$|{}^3 P_1\rangle = \left(\frac{2}{3}\right)^{1/2} |p_{1/2 s_{1/2}} 1^- \rangle - \left(\frac{1}{3}\right)^{1/2} |p_{3/2 s_{1/2}} 1^- \rangle. \quad (13)$$

<sup>29</sup> T. A. Brody and M. Moshinsky, *Tables of Transformation Brackets* (Monografias Del Instituto De Fisica, Mexico, 1960).

<sup>30</sup> The notation for the coupling of angular momentum is that of A. R. Edmonds, *Angular Momentum in Quantum Mechanics* (Princeton University Press, Princeton, New Jersey, 1957).

We find that

$$E_{^3P_1}(1^-) = \frac{1}{2}[{}^1I_1(1) + 2 {}^3I_0(1) + 3 {}^3I_1(1)]. \quad (14)$$

Since the spin-orbit splitting between the  $p_{1/2}$  and  $p_{3/2}$  S-P levels of the shell model is given by the difference of the H-F energies for the  $p_j$  particle, we can use Eqs. (6) and (11) to determine the size of this splitting:

$$V_{p_{1/2}}^{\text{H-F}} - V_{p_{3/2}}^{\text{H-F}} = \epsilon_{p_{1/2}} - \epsilon_{p_{3/2}} \equiv \epsilon \\ = \frac{1}{8}[6 {}^3I_1(0) + 9 {}^3I_1(1) - 15 {}^3I_1(2)]. \quad (15)$$

From Eqs. (12) and (14) we note that the splitting among the  ${}^3P_{0,1,2}$ ,  $T=0$  levels depends only on the difference between the values of  ${}^3I_1(\mathfrak{S})$ :

$$E(0^-) - E(1^-) = \frac{3}{2}[{}^3I_1(0) - {}^3I_1(1)], \\ E(1^-) - E(2^-) = \frac{3}{2}[{}^3I_1(1) - {}^3I_1(2)], \\ E(0^-) - E(2^-) = \frac{3}{2}[{}^3I_1(0) - {}^3I_1(2)]. \quad (16)$$

The splitting between the  $0^-$  and  $2^-$  states for  $T=1$  also depends only on the values of  ${}^3I_1(\mathfrak{S})$ :

$$E(0^-) - E(2^-) = \frac{1}{4}[4 {}^3I_1(0) + 3 {}^3I_1(1) - 7 {}^3I_1(2)]. \quad (17)$$

The splitting between the isospin multiplets is given by

$$E(2^-) - E(2^0) = \frac{1}{2}[{}^1I_0(0) - {}^1I_1(1) - {}^3I_0(1)] \\ + \frac{1}{4}[{}^3I_1(1) + {}^3I_1(2)]. \quad (18)$$

To find the  $1^-$ ,  $T=1$  states, we must diagonalize the interaction among the states  $|p_{1/2} s_{1/2} 1^- \rangle$  and  $|p_{3/2} s_{1/2} 1^- \rangle$ . The matrix to be diagonalized is

$$\begin{pmatrix} E_{1/2}(1^-) - \lambda(1^-) & V_{1/2 \ 3/2}(1^-) \\ V_{3/2 \ 1/2}(1^-) & E_{3/2}(1^-) - \lambda(1^-) \end{pmatrix} \\ \times \begin{pmatrix} \alpha_{1/2}(1^-) \\ \alpha_{3/2}(1^-) \end{pmatrix} = 0. \quad (19)$$

Thus, the new eigenvalues,  $\lambda_{\pm}(1^-)$ , are

$$\lambda_{\pm}(1^-) = \frac{1}{2}[E_{1/2}(1^-) + E_{3/2}(1^-) \pm \{[E_{1/2}(1^-) - E_{3/2}(1^-)]^2 + 4[V_{1/2 \ 3/2}(1^-)]^2\}^{1/2}]. \quad (20)$$

The new eigenstates are given by

$$(\alpha_{1/2}/\alpha_{3/2})_+ = -\frac{V_{1/2 \ 3/2}(1^-)}{E_{1/2}(1^-) - \lambda_+(1^-)} \\ = -\frac{E_{3/2}(1^-) - \lambda_+(1^-)}{V_{1/2 \ 3/2}(1^-)} = -(\alpha_{3/2}/\alpha_{1/2})_-, \quad (21)$$

where  $+$  and  $-$  denote the upper and lower  $1^-$ ,  $T=1$  states, respectively.

The  $E1$  transitions to the ground state occur only from the  ${}^1P_1$ ,  $T=1$  components of the above states, where

$$|{}^1P_1\rangle = (\sqrt{\frac{1}{3}})|p_{1/2} s_{1/2} 1^- \rangle + (\sqrt{\frac{2}{3}})|p_{3/2} s_{1/2} 1^- \rangle. \quad (22)$$

As an estimate of the ratio of the  $E1$  transition probabilities for the two  $1^-$ ,  $T=1$  states, we can calculate the ratio of the probabilities of finding the above states in the  ${}^1P_1$  configuration:

$$\frac{|\langle {}^1P_1 | \Psi_+ \rangle|^2}{|\langle {}^1P_1 | \Psi_- \rangle|^2} = \frac{|(\alpha_{1/2})_+ + \sqrt{2}(\alpha_{3/2})_+|^2}{|(\alpha_{1/2})_- + \sqrt{2}(\alpha_{3/2})_-|^2} \\ = \left| \frac{(\alpha_{1/2}/\alpha_{3/2})_+ + \sqrt{2}}{1 - \sqrt{2}(\alpha_{1/2}/\alpha_{3/2})_+} \right|^2. \quad (23)$$

For a better estimate, we can include the correct energy weighting for  $E1$  transitions, which goes as the energy difference cubed.

Using the definition of the center of gravity of the supermultiplet as given in SW, we find that

$$\epsilon_{\text{c.g.}} = \epsilon_p - \epsilon_s - \frac{1}{4}[{}^1I_0(0) + {}^3I_0(1)] \\ - (1/20)[{}^1I_1(1) + {}^3I_1(0) + 3 {}^3I_1(1) + 5 {}^3I_1(2)] \\ = \epsilon_p - \epsilon_s - \frac{1}{4}[{}^1I_0(0) + {}^3I_0(1)] \\ - \frac{1}{4}\{{}^1I_1(1) + \frac{1}{3}[{}^3I_1(0) + {}^3I_1(1) + {}^3I_1(2)]\} \\ + \frac{1}{5}\{{}^1I_1(1) + \frac{1}{6}[{}^3I_1(0) - 2 {}^3I_1(1) - 5 {}^3I_1(2)]\} \\ = \epsilon_p - \epsilon_s + v_{ps;ps}^{[15]} + \frac{1}{5}\{{}^1I_1(1) \\ + \frac{1}{6}[{}^3I_1(0) - 2 {}^3I_1(1) - 5 {}^3I_1(2)]\}, \quad (24)$$

where  $\epsilon_p - \epsilon_s$  is the difference in the particle-hole energies, which we take from experiment to be the oscillator spacing,  $\hbar\omega_0 = 21.8$  MeV.<sup>31</sup> In Eq. (24)

$$v_{ps;ps}^{[15]} = -\langle 1p1sL | V | 1p1sL \rangle_0 \\ = -\frac{1}{4}\{{}^1I_0(0) + {}^3I_0(1) + {}^1I_1(1) \\ + \frac{1}{3}[{}^3I_1(0) + {}^3I_1(1) + {}^3I_1(2)]\} \quad (25)$$

is the repulsive, spin-independent interaction of SW which moves the center of gravity of the supermultiplet upwards. The third term in Eq. (24) is caused by the spin-dependent forces and gives rise to an additional shift in the position of the center of gravity besides that predicted by the supermultiplet theory.

To determine the muon-capture matrix elements and the total capture rate in  ${}^4\text{He}$ , we use the formulas of deForest,<sup>32</sup> except that we couple  $(sl)j$ , instead of  $(ls)j$ . Thus the total capture rate is given by

$$\Lambda_{\mu c} = [\nu_{\mu}^2(|\phi_{\mu}|^2)_{\text{av}}/2\pi\hbar^2c][G_V^2 M_V^2 + 3G_A^2 M_A^2 \\ + (G_P^2 - 2G_F G_A)M_P^2] + \Lambda'_{\mu c}, \quad (26)$$

where the  $G$ 's are effective coupling constants, the  $M$ 's are the nuclear matrix elements,  $\Lambda_{\mu c}'$  contains nucleon recoil corrections and  $\nu_{\mu} \equiv m_{\mu}c/\hbar$ .

For  ${}^4\text{He}$  the dipole nuclear matrix elements, i.e.,

<sup>31</sup> One can also take the S-P energies from neighboring nuclei in which case  $\epsilon_p - \epsilon_s = 22.6$  MeV. Thus, all of our results for the center of gravity would be 0.8 MeV larger if we used this value of  $\epsilon_p - \epsilon_s$ .

<sup>32</sup> T. de Forest, Jr., Phys. Rev. **139**, B1217 (1965).

$(M_I^2)_D$ , where  $I=V,P,A$ , are given by

$$\begin{aligned} (M_V^2)_{D,J=1}^{(i)} &= \frac{1}{3} |f(\eta)_{J=1}^{(i)}|^2 (y_{J=1}^{(i)}/y_\mu) \\ &\quad \times |\alpha_{(i)}^{(01\ 1/2)(00\ 1/2)-1} + \sqrt{2}\alpha_{(i)}^{(01\ 3/2)(00\ 1/2)-1}|^2, \\ (M_P^2)_{D,J=0} &= \frac{1}{3} |f(\eta)_{J=0}|^2 (y_{J=0}/y_\mu) = 3(M_A^2)_{D,J=0}, \\ (M_P^2)_{D,J=2} &= \frac{2}{3} |f(\eta)_{J=2}|^2 (y_{J=2}/y_\mu) = 6/5(M_A^2)_{D,J=2}, \\ (M_P^2)_{D,J=1} &= \frac{1}{9} |f(\eta)_{J=1}^{(i)}|^2 (y_{J=1}^{(i)}/y_\mu) \\ &\quad \times \sqrt{2} |\alpha_{(i)}^{(01\ 1/2)(00\ 1/2)-1} - \alpha_{(i)}^{(01\ 3/2)(00\ 1/2)-1}|^2, \quad (27) \end{aligned}$$

where

$$f(\eta) = (\sqrt{6}) \int_0^\infty R_{01} j_1(\nu_{ab} r) R_{00} r^2 dr = \eta \exp(-\eta^2/4),$$

$\eta \equiv \nu_{ab} b_0 = |\mathbf{p}_{\nu_{ab}}| b_0/\hbar$ ,  $\nu_{ab} \equiv \mathbf{p}_\nu/\hbar$  is the neutrino wave number,  $y^{(i)} \equiv (\frac{1}{2}\nu_{ab}^{(i)} b_0)^2$ ,  $y_\mu \equiv (\frac{1}{2}\nu_\mu b_0)^2$ , and  $b_0$  is the oscillator parameter.

We also calculate the unretarded dipole matrix elements  $(M_I^2)_{UD}$  and the elastic form factor  $F_{el}(\nu_{res})$  evaluated at the resonant neutrino momentum  $\hbar\nu_{res}$  so that we can check the assumption of FW that

$$(M_I^2)_D = (M_I^2)_{UD} |F_{el}(\nu_{res})|^2. \quad (28)$$

In our calculation the unretarded dipole matrix elements are obtained from the retarded ones by replacing  $f(\eta)$  by  $\eta = \nu_{ab} b_0$  in Eq. (27). The elastic form factor, which we want for comparison, is the one uncorrected for center-of-mass motion<sup>33</sup> and given by<sup>28</sup>

$$F_{el}(\nu_{res}) = \exp(-\eta^2/4), \quad (29)$$

where  $\eta = \nu_{res} b_0$ .

### III. CALCULATIONS AND NUMERICAL RESULTS

#### A. The Tabakin Separable Potential

Since the Tabakin potential is nonsingular and separable and has been determined for relative  $s$ -,  $p$ -, and  $d$ -state interactions, it is a convenient realistic nucleon-nucleon potential with which to make a consistent calculation of the spectrum of the  $\alpha$  particle. For convenience in doing integrals we calculate matrix elements of the separable potential in momentum space. The Tabakin potential in momentum space is given by

$$\begin{aligned} V(\mathbf{k}|\mathbf{k}') &= (2\hbar^2/\pi M) \sum_{\alpha m l l'} i^{l'-l} [-g_{\alpha l}(k)g_{\alpha l'}(k') \\ &\quad + h_{\alpha l}(k)h_{\alpha l'}(k')] \mathcal{Y}_{\alpha l}^m(\hat{\mathbf{k}}) \mathcal{Y}_{\alpha l'}^{m*}(\hat{\mathbf{k}}'), \quad (30) \end{aligned}$$

<sup>33</sup> If we evaluated  $(M_I^2)_D$  for the true wave functions for the  $J^\pi$ ,  $T=1$  states, then  $(M_I^2)_{UD}^{true} = (M_I^2)_{UD} |F_{el}^{true}|^2$ , where  $F_{el}^{true}$  is the elastic form factor corrected for center-of-mass motion as described in L. J. Tassie and F. C. Barker, Phys. Rev. **111**, 940 (1958). However, we evaluate  $(M_I^2)_D$  for harmonic-oscillator shell-model wave functions. Thus  $(M_I^2)_D^{SM} = (M_I^2)_{UD} |F_{el}^{SM}|^2$ , where  $F_{el}^{SM}$  is the elastic form factor *uncorrected* for center-of-mass motion, since for shell-model wave functions the same center-of-mass contribution factors out of  $(M_I^2)_D$  and  $|F_{el}|^2$  and cancels. In both cases  $(M_I^2)_{UD}$  is unaffected by the center-of-mass motion, since it is evaluated for  $\nu_{ab} \rightarrow 0$ .

TABLE II. Parameters of the Tabakin separable potential.

State	$V_\gamma$ (MeV)	$V_\beta$ (MeV)	$1/a$ (F)	$1/b$ (F)	$1/c$ (F)	$1/d$ (F)
$^1S_0$	115.9	235.6	0.834	0.801	...	0.694
$^3S_1$	164.7	10.3	0.763	0.990	...	0.590
$^3D_1$	189.3	488.9	0.833	0.909	2.00	...
$^1P_1$	44.3	1506.0	0.741	0.741	...	...
$^3P_0$	267.7	1067.0	0.714	0.714	...	...
$^3P_2$	103.7	394.5	0.625	0.625	...	...
$^3P_1$	107.6	531.2	0.800	0.800	...	...

where  $\hbar\mathbf{k}$  is the relative momentum,  $\alpha$  stands for the quantum numbers  $\mathfrak{S}$ ,  $T$ , and  $S$ , as defined earlier, and  $m$  is the  $z$  component of  $\mathfrak{S}$ .  $\mathcal{Y}_{\alpha l}^m(\hat{\mathbf{k}})$  is defined by

$$\mathcal{Y}_{\alpha l}^m(\hat{\mathbf{k}}) = \sum_{m_l m_s} (l m_l S m_s | l S \mathfrak{S} m) Y_{l m_l}(\hat{\mathbf{k}}) \chi_{S m_s} P_T, \quad (31)$$

where  $Y_{l m_l}$  is a spherical harmonic,  $\chi_{S m_s}$  is the spin wave function,  $P_T$  is the isotopic spin projection operator, and  $(l m_l S m_s | l S \mathfrak{S} m)$  is the Clebsch-Gordan coefficient for coupling  $l$  and  $S$  to give  $\mathfrak{S}$ . The functions  $g_{\alpha l}(k)$  are as follows:

$$\begin{aligned} ^1S_0: \quad & \alpha = (0,1,0), \\ & g_{\alpha 0}(k) = \gamma(k^2 + a^2)^{-1}, \\ & h_{\alpha 0}(k) = \beta k^2 [(k-d)^2 + b^2]^{-1} [(k+d)^2 + b^2]^{-1}. \\ ^3S_1: \quad & \alpha = (1,0,1), \\ & g_{\alpha 0}(k) = \gamma(k^2 + a^2)^{-1}, \\ & h_{\alpha 0}(k) = \beta k^2 [(k-d)^2 + b^2]^{-1} [(k+d)^2 + b^2]^{-1}. \\ ^3D_1: \quad & \alpha = (1,0,1), \\ & g_{\alpha 2}(k) = \gamma k^2 [(k-c)^2 + a^2]^{-1} [(k+c)^2 + a^2]^{-1}, \\ & h_{\alpha 2}(k) = \beta k^2 (k^2 + b^2)^{-2}. \\ ^3P_0: \quad & \alpha = (0,1,1), \\ & g_{\alpha 1}(k) = \gamma k (k^2 + a^2)^{-3/2}, \\ & h_{\alpha 1}(k) = \beta k^3 (k^2 + b^2)^{-5/2}. \end{aligned}$$

The functions  $g_{\alpha l}$  and  $h_{\alpha l}$  for  $^3P_1$ ,  $^3P_2$  and  $^1P_1$  are of the same form as those for  $^3P_0$ , except that for  $^3P_1$  and  $^1P_1$  the terms involving *both*  $g_{\alpha l}$  and  $h_{\alpha l}$  are taken to be positive, while for  $^3P_2$  *both* are taken to be negative. Otherwise, the signs are as indicated in Eq. (30). The parameters for the Tabakin potential are given in Table II, where  $V_\gamma = \hbar^2 \gamma^2 / M a$  and  $V_\beta = \hbar^2 \beta^2 / M b$ .

For the Tabakin potential we find that<sup>16</sup>

$$\begin{aligned} \langle (n' l' S) \mathfrak{S} T | V | (n l S) \mathfrak{S} T \rangle_0 &= \rho G_{n' l' S}(\mathfrak{S} T) G_{n l S}(\mathfrak{S} T) \\ &\quad + \zeta H_{n' l' S}(\mathfrak{S} T) H_{n l S}(\mathfrak{S} T) \\ &= {}^S I_l(\mathfrak{S}), \quad \text{for } l=l' \text{ and } n=n'=0, \quad (32) \end{aligned}$$

where  $\rho$  and  $\zeta$  are the correct relative signs for the interactions as explained earlier and

$$G_{n l S}(\mathfrak{S} T) = (2\hbar^2/\pi M)^{1/2} \int_0^\infty g_{\alpha l}(k) P_{n l}(k) k^2 dk, \quad (33)$$

$$H_{n l S}(\mathfrak{S} T) = (2\hbar^2/\pi M)^{1/2} \int_0^\infty h_{\alpha l}(k) P_{n l}(k) k^2 dk. \quad (34)$$

TABLE III. Matrix elements for  ${}^4\text{He}$  using the Tabakin separable potential.

$n$	$l$	State			$G_{nlS}(\mathfrak{S}T)$ (MeV) $^{1/2}$	$H_{nlS}(\mathfrak{S}T)$ (MeV) $^{1/2}$	$\langle(nlS)\mathfrak{S}T V (nlS)\mathfrak{S}T\rangle_0$ (MeV)	Second-order correction (%)
		$S$	$\mathfrak{S}$	$T$				
0	0	0	0	1	3.116	0.530	-9.428	+11.5
1	0	0	0	1	2.436	1.365	-4.068	
0	0	1	1	0	3.403	0.110	-11.569	+25.4
1	0	1	1	0	2.806	0.319	-7.772	
0	2	1	1	0	1.916	3.684	+9.903	
0	1	0	1	0	1.075	2.090	+5.524	-27.4
1	1	0	1	0	1.020	3.365	+12.366	
0	1	1	0	1	2.498	1.599	-3.684	+2.1
1	1	1	0	1	2.430	2.641	+1.070	
0	1	1	1	1	1.874	1.501	+5.763	-17.0
1	1	1	1	1	1.681	2.286	+8.051	
0	1	1	2	1	1.256	0.676	-2.033	+10.1
1	1	1	2	1	1.327	1.216	-3.242	

$P_{nl}(k)$  is the same as  $R_{nl}(r)$ , the radial part of the harmonic-oscillator wave function, except that  $r$  is replaced by  $k$  and there is an extra factor of  $(-1)^n$ . The notation for  $R_{nl}$  and  $P_{nl}$  is that of Brody and Moshinsky,<sup>29</sup> and  $n$  starts at zero instead of one.

From the work of Tabakin in nuclear matter<sup>10</sup> we know that the second-order contributions to the  $t$  matrix can be relatively large, particularly for the  ${}^3S_1+{}^3D_1$  interaction. Since we are interested in eventually solving for nuclear spectra using the  $t$  matrix, it is worthwhile to look at second-order effects, especially for the Tabakin potential which makes the calculations straightforward. To second order the  $t$  matrix for the particle-particle interaction is given by

$$\langle(nlS)\mathfrak{S}T|t|(nlS)\mathfrak{S}T\rangle_0 \stackrel{\text{second}}{\text{order}} = \langle(nlS)\mathfrak{S}T|V|(nlS)\mathfrak{S}T\rangle_0 + \sum'_{n'l'} \frac{|\langle(n'l'S)\mathfrak{S}T|V|(nlS)\mathfrak{S}T\rangle_0|^2}{E(nl) - E(n'l')}, \quad (35)$$

where  $\sum'$  means  $n' \neq n$  and  $l' \neq l$ .

In order to conserve parity, we must sum over states of an even number of excitations. Thus, since  $N$  and  $\mathcal{Q}$  for the center of mass must remain the same, the smallest energy denominator in the sum is  $-2\hbar\omega_0 = -43.6$  MeV. Since this is a large number and since the next smallest denominator is  $-4\hbar\omega_0 = -87.2$  MeV, we neglect all higher order excitations and keep only double excitations in the sum. Hence, Eq. (35) for the Tabakin potential takes the form

$$\langle(nlS)\mathfrak{S}T|t|(nlS)\mathfrak{S}T\rangle_0 \stackrel{\text{second}}{\text{order}} = \rho[G_{nlS}(\mathfrak{S}T)]^2 + \dagger[H_{nlS}(\mathfrak{S}T)]^2 - \frac{1}{43.6 \text{ MeV}} \times \sum_{n'l'} [\rho G_{n'l'S}(\mathfrak{S}T)G_{nlS}(\mathfrak{S}T) + \dagger H_{n'l'S}(\mathfrak{S}T)H_{nlS}(\mathfrak{S}T)]^2. \quad (36)$$

Since  $n=0$  and  $l=0$  or  $1$  for the alpha particle, the pos-

sible values of  $n'$  and  $l'$  are  $n'=0, l'=3$  or  $n'=1, l'=1$  for  $l=1$ , and  $n'=0, l'=2$  or  $n'=1, l'=0$  for  $l=0$ . The values of  $G_{nlS}(\mathfrak{S}T)$  and  $H_{nlS}(\mathfrak{S}T)$  for the alpha particle are given in Table III along with the percentage correction in second order for the appropriate terms.<sup>34</sup> Our results for  ${}^8I_1(\mathfrak{S})$  using the Tabakin potential in first and second order are given in Table VII.

### B. Other Realistic Nucleon-Nucleon Potentials

For the purpose of comparison we also carry out our calculation with two singular, hard-core potentials.

1. The Brueckner-Gammel-Thaler (BGT) potential with a hard core has the form<sup>4</sup>

$$V(r) = ({}^1V_+{}^1P + {}^3V_+{}^3P) \left( \frac{1 - P_{12}^M}{2} \right) + ({}^1V_-{}^1P + {}^3V_-{}^3P) \left( \frac{1 - P_{12}^M}{2} \right),$$

$${}^1V = {}^1V^c(r),$$

$${}^3V = {}^3V^c(r) + {}^3V^t(r)S_{12} + {}^3V^s(r)\mathbf{I} \cdot \mathbf{S},$$

$$V(r) = V_0 e^{-\mu r} / \mu r, \quad r > D$$

$$= +\infty, \quad r < D, \quad (37)$$

where  $P_{12}^M$  is the Majorana exchange operator,  $S_{12} = 3(\boldsymbol{\sigma}_1 \cdot \hat{r})(\boldsymbol{\sigma}_2 \cdot \hat{r}) - (\boldsymbol{\sigma}_1 \cdot \boldsymbol{\sigma}_2)$  is the tensor operator, and  ${}^1P, {}^3P$  are the singlet and triplet projection operators, respectively. The parameters  $\mu$  and  $V_0$  are listed in Table IV.

<sup>34</sup> Since Tabakin does not give a potential for relative  $f$  states, we estimated its effect on the triplet  $p, \mathfrak{S}=2$  state, the only state it influences, by the average value of the overestimated and underestimated values of

$$\langle(031)21|{}^3V_-|(011)21\rangle_0 = \langle(031)21|{}^3V^t S_{12}|(011)21\rangle_0 = 6(6/35)^{1/2} {}^3I_2^t$$

calculated for the BGT potential. Its contribution was found to be small as expected, about 3% of  ${}^3I_1^2$  in first order, and is included in the result in Table III.

TABLE IV. Parameters for the Brueckner-Gammel-Thaler potential.<sup>a</sup>

State	$V_0$ (MeV)	$\mu$ (F <sup>-1</sup> )
$^1V_{+c}$	-434.0	1.45
$^3V_{+c}$	-877.39	2.0908
$^3V_{+t}$	-159.40	1.0494
$^3V_{+tS}$	-5000	3.70
$^1V_{-c}$	+130.0	1.00
$^3V_{-c}$	-14.0	1.00
$^3V_{-t}$	+22.0	0.80
$^3V_{-tS}$	-7315	3.70

<sup>a</sup> The hard-core radius  $D=0.4$  F.

2. The Hamada potential<sup>26</sup> with a hard core has the same form as the BGT potential, except that  $^1V$  and  $^3V$  each have an extra term and the radial dependence is different, as indicated below:

$$^1V = ^1V^c(r) + ^1V^q(r)Q_{12},$$

$$^3V = ^3V^c(r) + ^3V^t(r)S_{12} + ^3V^{tS}(r)\mathbf{I}\cdot\mathbf{S} + ^3V^q(r)Q_{12}, \quad (38)$$

where  $Q_{12} = (\boldsymbol{\sigma}_1 \cdot \mathbf{l})(\boldsymbol{\sigma}_2 \cdot \mathbf{l})$  is the quadratic spin-orbit operator. For the central and  $Q$  potentials

$$V(r) = G\mu Y(\mu r) \{1 + AY(\mu r) + B[Y(\mu r)]^2\},$$

where  $Y(x) = e^{-x}/x$  and  $\mu$  is the pion mass. The tensor potentials are given by

$$V^t(r) = G\mu Y(\mu r) \{1 + (3/\mu r) + [3/(\mu r)^2]\} \\ \times \{1 + AY(\mu r) + B[Y(\mu r)]^2\}$$

and the spin-orbit potentials by

$$V^{tS}(r) = G\mu [Y(\mu r)]^2 [1 + AY(\mu r)].$$

All of these potentials are for  $r > D$ ; for  $r < D$  they are all infinite, where  $D$  is the core radius. The parameters for the Hamada potential are given in Table V.

For both of these potentials we immediately observe that the tensor and spin-orbit forces act *only* in the  $l=1$ ,  $S=1$  state, since both of these interactions are zero if either  $l$  or  $S$  is zero. Hence, for these potentials

$$\langle (00S)ST | ^S V | (00S)ST \rangle_0 = ^S I_0(S) = ^S I_0, \quad (39)$$

where  $^S I_0$  is the Talmi integral,

$$^S I_l = \frac{2}{\Gamma(l + \frac{3}{2})} \int_0^\infty e^{-x^2} ^S V(\bar{b}_0 x) x^{2l+2} dx \quad (40)$$

for  $l=0$ , and  $\bar{b}_0 = \sqrt{2}b_0 = 1.95$  F for  $^4\text{He}$ . Also

$$\langle (01S)\mathfrak{S}T | V | (01S)\mathfrak{S}T \rangle_0 = ^S I_1(\mathfrak{S}) = ^S I_1^c \\ + \delta(S=1)\delta(\mathfrak{S}=J) \left\{ (-1)^{J+1} 12 \begin{Bmatrix} J & 1 & 1 \\ 2 & 1 & 1 \end{Bmatrix} \right\} \\ + (-1)^J 6 \begin{Bmatrix} J & 1 & 1 \\ 1 & 1 & 1 \end{Bmatrix} ^3 I_1^{tS} \\ + \left[ \frac{2}{3} + (-1)^J 10 \begin{Bmatrix} J & 1 & 1 \\ 2 & 1 & 1 \end{Bmatrix} \right] ^3 I_1^q \}, \quad (41)$$

TABLE V. Parameters for the Hamada potential.

State	$G$	$A$	$B$	$D\mu$ (core)
$^1V_{+c}$	-0.08	10.0	8.0	0.337
$^1V_{+Q}$	-0.00155	8.0	6.0	0.337
$^3V_{+c}$	-0.08	-8.0	4.0	$0.275 + 0.00144 [E \text{ (MeV)}]^{1/2}$
$^3V_{+Q}$	-0.007445	12.0	2.0	$0.275 + 0.00144 [E \text{ (MeV)}]^{1/2}$
$^3V_{+t}$	-0.08	-0.4	0.1	$0.275 + 0.00144 [E \text{ (MeV)}]^{1/2}$
$^3V_{+tS}$	0.05956	4.0	...	$0.275 + 0.00144 [E \text{ (MeV)}]^{1/2}$
$^1V_{-c}$	0.24	3.0	-1.0	0.30
$^1V_{-Q}$	0	0	0	0.30
$^3V_{-c}$	0.0267	-9.0	4.6	0.320
$^3V_{-Q}$	0.00045	10.0	6.0	0.320
$^3V_{-t}$	0.0267	-1.14	0.2	0.320
$^3V_{-tS}$	0.1541	-8.09	...	0.320

where the superscripts refer to the appropriate components of the interaction. The  $Q$  term, of course, appears only for the Hamada potential. In particular we note that

$$^3 I_1(0) = ^3 I_1^c - 4 ^3 I_1^t - 2 ^3 I_1^{tS} + 4 ^3 I_1^q, \\ ^3 I_1(1) = ^3 I_1^c + 2 ^3 I_1^t - ^3 I_1^{tS} - ^3 I_1^q, \\ ^3 I_1(2) = ^3 I_1^c - \frac{2}{5} ^3 I_1^t + ^3 I_1^{tS} + ^3 I_1^q, \quad (42)$$

so that upon substitution into Eq. (15), we find that

$$\epsilon = -(9/2) ^3 I_1^{tS}. \quad (43)$$

Therefore, in first order the spin-orbit splitting of the shell model is caused by the relative spin-orbit interaction of the nucleon-nucleon potential.

Substituting Eq. (42) into Eqs. (16) and (17), we find that

$$E(0-0) - E(2-0) = -\frac{9}{2} ^3 I_1^{tS} - (27/5) ^3 I_1^t + \frac{9}{2} ^3 I_1^q, \\ E(0-0) - E(1-0) = -\frac{9}{2} ^3 I_1^{tS} - 9 ^3 I_1^t + (15/2) ^3 I_1^q, \\ E(1-0) - E(2-0) = -3 ^3 I_1^{tS} + (18/5) ^3 I_1^t - 3 ^3 I_1^q, \\ E(0-1) - E(2-1) = -\frac{9}{2} ^3 I_1^{tS} - (9/5) ^3 I_1^t + \frac{9}{2} ^3 I_1^q. \quad (44)$$

Equation (44) clearly indicates how these four splittings depend upon the different components of the two-body interaction.

We also observe that

$$^3 I_1(0) + 3 ^3 I_1(1) + 5 ^3 I_1(2) = 9 ^3 I_1^c + 6 ^3 I_1^q, \quad (45)$$

so that the center of gravity of the supermultiplet, as given by Eq. (24), is independent of the tensor and spin-orbit interactions.

In making calculations with the singular hard-core potentials, we must determine how to treat the core. DTW showed that the contribution of the hard-core part of the potential to the two-body matrix element for

TABLE VI. Parameters for the nonsingular potentials.

Well shape	State	$V_0$ (MeV)	$\mu$ (F <sup>-1</sup> )
Yukawa: $V_0 e^{-\mu r}/\mu r$	Singlet	-46.87	0.8547
	Triplet	-52.13	0.7261
Exponential: $V_0 e^{-\mu r}$	Singlet	-108.0	1.409
	Triplet	-192.7	1.506

TABLE VII.  ${}^sI_l(\mathfrak{S})$  for all potentials discussed in this paper. Also Talmi integrals for components of the potential where applicable. All  $T$ 's are in MeV. Note:  ${}^1I_1^q=0$ .

Potentials	${}^1I_0(0)$ $T=1$	${}^3I_0^c$ $T=0$	${}^3I_0^t$ $T=0$	${}^3I_0^{ls}$ $T=0$	${}^3I_0(1)$ $T=0$	${}^1I_1(1)$ $T=0$	${}^3I_1^c$ $T=1$	${}^3I_1^t$ $T=1$	${}^3I_1^{ls}$ $T=1$	${}^3I_1^q$ $T=1$	${}^3I_1(0)$ $T=1$	${}^3I_1(1)$ $T=1$	${}^3I_1(2)$ $T=1$
A. Tabakin:													
1. First order	- 9.43	-11.57			-11.57	+ 5.52	+0.38	+1.85	-1.67		-3.68	+5.76	-2.03
2. Second order	-10.51	-14.50			-14.50	+ 4.01	-0.076	+1.67	-1.49		-3.76	+4.77	-2.24
B. Others:													
1. BGT <sup>a</sup>	-17.30	-11.40	-12.93	-9.20	-11.40	+ 5.51	-0.59	+1.71	-2.23		-2.97	+5.06	-3.50
2. BGT <sup>b</sup>	- 4.72	- 0.67	- 4.14	+2.00	- 0.67	+ 2.97	-0.32	+1.01	-0.37		-3.62	+2.07	-1.09
3. BGT <sup>c</sup>	-11.01	- 6.04	- 8.58	-3.60	- 6.04	+ 4.24	-0.46	+1.36	-1.30		-3.30	+3.56	-2.30
4. Hamada <sup>d</sup>						+ 5.93	-0.29	+1.27	-2.43	+0.032	-0.38	+4.65	-3.20
5. Hamada <sup>e</sup>						+ 2.97	-0.016	+0.75	-0.20	+0.010	-2.60	+1.68	-0.50
6. Hamada <sup>f</sup>						+ 4.45	-0.15	+1.01	-1.31	+0.021	-1.49	+3.16	-1.85
7. Yukawa well	- 9.34	-14.29			-14.29								
8. Exponential well	- 9.81	-15.33			-15.33								
9. Mitra <i>et al.</i>	- 9.68	-12.56			-12.56	+24.04					+5.40	+2.70	-2.70

<sup>a</sup> BGT potential with Moshinsky hard core for  $l=0$ . Overestimate.  
<sup>b</sup> BGT potential with Moshinsky hard core for  $l=0$ . Underestimate.  
<sup>c</sup> BGT potential with Moshinsky hard core for  $l=0$ . Average of overestimated and underestimated values.  
<sup>d</sup> Hamada potential for  $l=1$  only. Integrals cut off at core radius. Overestimate.  
<sup>e</sup> Hamada potential for  $l=1$  only. Underestimate.  
<sup>f</sup> Hamada potential for  $l=1$  only. Average of overestimated and underestimated values.

$l>0$  should be small relative to the noncore contribution. Therefore, they neglected the effect of the core on  $I_l$  for  $l>0$  and calculated these Talmi integrals by using ordinary perturbation theory for the attractive part of the potential and cutting off the integrals at the core radius. We calculate our Talmi integrals for  $l>0$  in the same manner.

However, for  $l=0$  we cannot neglect the effect of the hard core. DTW handled the hard core in  $s$  states in several ways. They first identified the  $s$ -state Talmi integrals with the energy shifts from the harmonic-oscillator energy eigenvalues for  $l=0$ . They then calculated the energy shifts by solving the relative Schrödinger equation by both a variational method and numerical integration on a computer. They also computed  $I_0$  directly by using perturbation theory for the attractive well and the Moshinsky potential<sup>35</sup> for the hard core. In first order the Moshinsky potential consists of replacing the hard core by a delta-function pseudopotential

$$V_C \rightarrow 2\pi\hbar\omega(D/\bar{b}_0)\delta[(\mathbf{r}_1-\mathbf{r}_2)/\bar{b}_0]. \quad (46)$$

We use this latter method in computing our  $s$ -state Talmi integrals for the BGT potential. We do not calculate  $I_0$  for the Hamada potential.

For both  $l=0$  and 1 we calculate what we call an overestimate and an underestimate of the Talmi integral. The overestimate is obtained by cutting off the integral at the core radius, while the underestimate is determined by shifting the potential well to the origin and then integrating from zero to infinite.

We also calculate  $I_0$  for the usual nonsingular Yukawa and exponential nucleon-nucleon potentials, since Dawson

and Walecka showed that these potentials give *essentially the same results* as the more sophisticated BGT and Hamada potentials. The parameters for these nonsingular potentials are given in Table VI.<sup>36</sup>

Our results for  ${}^sI_l(\mathfrak{S})$  computed with the two singular and the two nonsingular potentials are recorded in Table VII. We note that the values of  ${}^3I_1^c$ ,  ${}^3I_1^t$ , and  ${}^3I_1^{ls}$  for the Tabakin potential come from setting  ${}^3I_1^q=0$  in Eq. (42) and solving these three equations for the Talmi integrals, using the calculated values of  ${}^3I_1(0)$ ,  ${}^3I_1(1)$  and  ${}^3I_1(2)$ .

We also perform our calculation with the separable potential of Mitra *et al.*<sup>27</sup> However, the results for the relative  $p$  states are obviously too large. Thus, we do not use these results in plotting the spectrum of  ${}^4\text{He}$ , although we do include the values of  ${}^sI_l(\mathfrak{S})$  we obtain in Table VII.<sup>37</sup>

We plot the spectrum of the alpha particle for four cases:

- (1) The Tabakin potential in second order.
- (2) The Tabakin potential in first order.
- (3) A Yukawa well in  $s$  states (as justified by the results of Dawson and Walecka), since the  $s$  state contributions are doubtful for the singular potentials, and all  ${}^sI_l(\mathfrak{S})$ 's determined from an average of the underestimated and overestimated values calculated for the Hamada potential.

<sup>36</sup> L. Hulthén and M. Sugawara, in *Handbuch der Physik*, edited by S. Flügge (Springer-Verlag, Berlin, 1957), Vol. 39, pp. 52, 62.

<sup>37</sup> The form of the Mitra *et al.* separable potential and its parameters are given in Ref. (27) and in other references given therein. We agree with the statement of V. L. Narasimham, S. K. Shah, and S. P. Pandya, [Nucl. Phys. 33, 529 (1962)] that the  $p$ -state potentials are in doubt and need to be checked. In a recent article on the trineutron, A. N. Mitra and V. S. Bhasin [Phys. Rev. Letters 16, 523 (1966)] propose a new form for the triplet  $p$  potential.

<sup>35</sup> M. Moshinsky, Rev. Mex. Fis. 6, 185 (1957); M. Bauer and M. Moshinsky, Nucl. Phys. 4, 615 (1957).

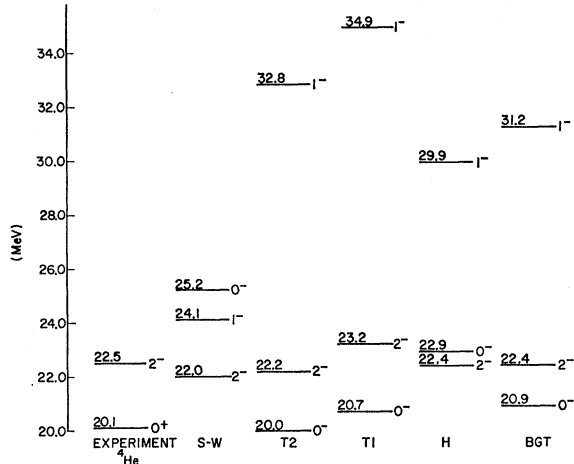


FIG. 1.  $T=0$  spectrum of  ${}^4\text{He}$  for (a) experiment,  ${}^4\text{He}$ ; (b) S-W, de-Shalit and Walecka, Ref. 25; (c) T2, Tabakin potential in second order; (d) T1, Tabakin potential in first order; (e) H, Hamada potential (average) in  $p$  states and a Yukawa well in  $s$  states; (f) BGT, BGT potential in  $p$  states and a Yukawa well in  $s$  states.

(4) A Yukawa well in  $s$  states and all  ${}^sI_1(\mathfrak{F})$ 's determined from an average of the underestimated and overestimated values calculated for the BGT potential.

These plots are shown in Figs. 1 and 2 along with the experimental levels<sup>38</sup> and the results of SW for comparison.

From Fig. 2 it is apparent that our calculated values for the intrinsic splittings are too large. The reason they are too big is that we have overestimated the contribution of the relative  $p$ -state interaction by performing our calculation with harmonic-oscillator wave functions, when the excited states of the  $\alpha$  particle are actually in

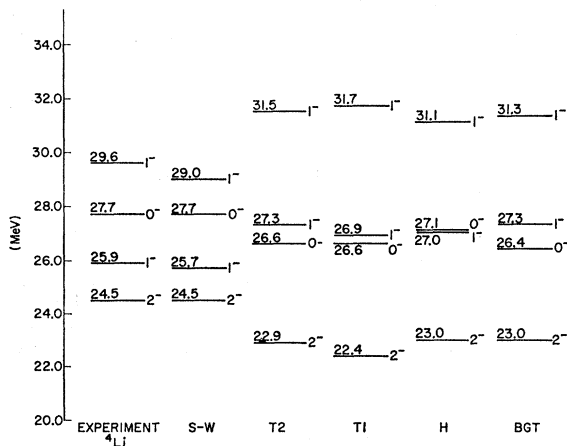


FIG. 2.  $T=1$  spectrum of  ${}^4\text{He}$  for the same cases as in Fig. 1, except that the experimental levels are from  ${}^4\text{Li}$ .

<sup>38</sup> When plotting the experimental spectrum of  ${}^4\text{He}$ , we used the data of Meyerhof [Ref. (40)] which shows the  $2^-, T=0$  state at 22.5 MeV. In Ref. 25, de-Shalit and Walecka took the  $2^-, T=0$  to be located at 22.0 MeV.

the continuum. To determine the effect of decreasing the overlap in the  $p$  states, we calculate the  $I$ 's and the spectrum using the Tabakin potential for increasing values of the oscillator parameter. As SW showed, the same oscillator parameter must be used in the ground state and the negative-parity states, otherwise one encounters tremendous problems in correctly treating the center-of-mass motion. Consequently, we also vary  $b_0$  in the relative  $s$  states, so that all calculations for a given set of splittings are determined for the same value of  $b_0$ . The results of this calculation for the Tabakin potential in second order are shown in Figs. 3-6.

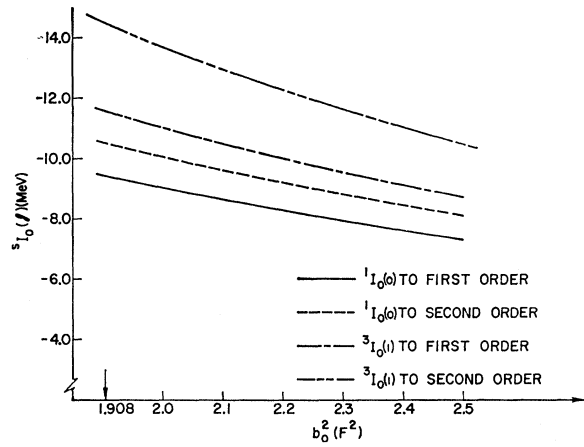


FIG. 3.  ${}^sI_0(\mathfrak{F})$ , calculated using the Tabakin potential for increasing values of  $b_0^2$ . The arrow marks the values of  $b_0^2$  used in our calculation of the spectrum in Figs. 1 and 2.

The calculated values of  $\epsilon = \epsilon_{p1/2} - \epsilon_{p3/2}$  for the different potentials are given in Table VIII, and the computed values of the center of gravity are listed in Table IX. SW obtained a value of  $\epsilon_{c.g.}$  (experimental) = 25.8 MeV, by assuming the Landé interval rule to be true for the unobserved  $0^-$  and  $1^-, T=0$  states. According

TABLE VIII.  $\epsilon_{p1/2} - \epsilon_{p3/2}$  calculated from the difference in the Hartree-Fock energies.

	$\epsilon_{p1/2} - \epsilon_{p3/2} = -(9/2) {}^sI_1^{LS}$ (MeV)
A. Tabakin potential	
1. Second order	6.7
2. First order	7.5
B. Other potentials	
1. Hamada (overestimate)	10.9
2. Hamada (underestimate)	0.9
3. Hamada (average)	5.9
4. BGT (overestimate)	10.0
5. BGT (underestimate)	1.7
6. BGT (average)	5.8
7. Mitra <i>et al.</i> (separable)	12.2
C. Experimental result	
1. $p$ - $\alpha$ and $n$ - $\alpha$ scattering	$\sim 4$
2. ${}^4\text{He}$ (Ref. 46)	$2.6 \pm 0.4$

TABLE IX. Predictions for the center of gravity ( $\epsilon_{c.g.}$ ) of the supermultiplet (all in MeV).

	$\epsilon_p - \epsilon_s$	$-\frac{1}{4}[{}^1I_0(0) + {}^3I_0(1)]$	$-\frac{1}{20}[{}^1I_1(1) + {}^3I_1(0) + 3{}^3I_1(1) + 5{}^3I_1(2)]$	$\epsilon_{c.g.}$
A. Tabakin potential				
1. Second order	21.8 <sup>a</sup>	6.3	-0.2	27.9
2. First order	21.8	5.2	-0.4	26.6
B. Other potentials				
1. Hamada (overestimate)	21.8	5.9 <sup>b</sup>	-0.2	27.5
2. Hamada (underestimate)	21.8	5.9	-0.1	27.6
3. Hamada (average)	21.8	5.9	-0.2	27.5
4. BGT (overestimate)	21.8	5.9	-0.01	27.7
5. BGT (underestimate)	21.8	5.9	-0.00	27.7
6. BGT (average)	21.8	5.9	-0.01	27.7
7. Mitra <i>et al.</i> (separable)	21.8	5.6	-1.4	26.0

<sup>a</sup> From  $\hbar\omega_0$  as determined from electron scattering.

<sup>b</sup> From using a Yukawa well in  $s$  states. For B.1-6 only.

to our calculations, this is not correct. Assuming the  $T=0$  states to be split as indicated in Fig. 1, we find

$$\begin{aligned} \epsilon_{c.g.}(\text{experimental}) &= 26.3 \text{ MeV for the Tabakin potential} \\ &\quad \text{(first and second order)} \\ &= 26.2 \text{ MeV for the average of the} \\ &\quad \text{Hamada potential} \\ &= 26.1 \text{ MeV for the average of the} \\ &\quad \text{BGT potential. (47)} \end{aligned}$$

The predicted values of the levels shown in Figs. 1, 2, 5, and 6 are obtained by fitting the splittings we calculate to the appropriate experimental value of  $\epsilon_{c.g.}$  given in Eq. (47). If we had used our calculated values of

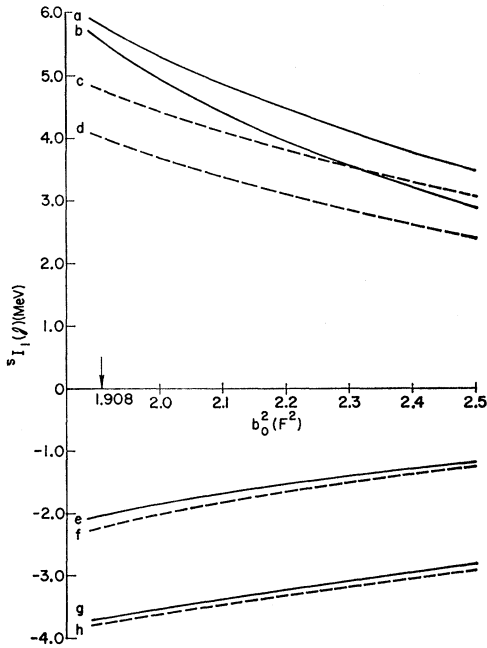


FIG. 4.  ${}^sI_1(J)$ , calculated using the Tabakin potential, for increasing values of  $b_0^2$ . The arrow has the same meaning as in Fig. 3. (a)  ${}^3I_1(1)$  to first order, (b)  ${}^1I_1(1)$  to first order, (c)  ${}^3I_1(1)$  to second order, (d)  ${}^1I_1(1)$  to second order, (e)  ${}^3I_1(2)$  to first order, (f)  ${}^1I_1(2)$  to second order, (g)  ${}^3I_1(0)$  to first order, (h)  ${}^1I_1(0)$  to second order.

TABLE X. Ratios of the coefficients for the  $1^-, T=1$  states in  ${}^4\text{He}$  and estimates of the ratio of the  $E1$  transition probabilities, with and without the energy weighting factor.

	$\frac{(\alpha_{1/2}/\alpha_{3/2})_+}{-(\alpha_{1/2}/\alpha_{1/2})_-}$ (a)	$P$ (b)	$(\Delta E_+/\Delta E_-)^2 P$
A. Tabakin potential			
1. Second order	5.39	1.06	1.58
2. First order	10.6	0.74	1.10
B. Other potentials			
1. Hamada (average)	2.39	2.54	3.79
2. BGT (average)	2.61	2.30	3.44
C. Comparison			
1. Serber force-Yukawa well (Ref. 25)	2.47	2.41	3.60
2. Experiment (Ref. 40)			$\sim 0.50$

<sup>a</sup> + denotes upper  $1^-, T=1$  state. - denotes lower  $1^-, T=1$  state.

<sup>b</sup>  $P = |\langle P_1|\psi_+\rangle|^2 / |\langle P_1|\psi_-\rangle|^2$ .

$\epsilon_{c.g.}$ , as given in Table IX, all of our levels would be pushed up by approximately  $\frac{3}{2}$  MeV.

In Table X we list the ratios of the coefficients for the  $1^-, T=1$  states caused by the configuration mixing.

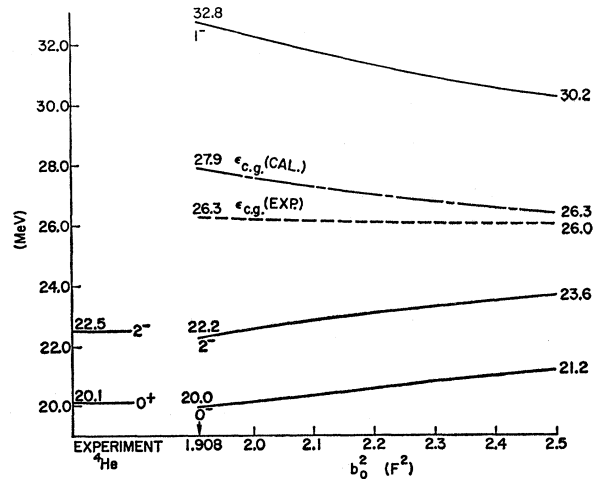


FIG. 5.  $T=0$  spectrum of  ${}^4\text{He}$ , determined from the Tabakin potential in second order, for increasing values of  $b_0^2$ . Also the calculated and experimental values of  $\epsilon_{c.g.}$  for increasing  $b_0^2$ . The arrow has the same meaning as in Fig. 3.

TABLE XI. Energies and wave functions for  $J^-, T=1$  states in  ${}^4\text{He}$ .

$T=1$ $J$	$E$ (MeV)	Tabakin potential (second order), calculated energies		$E$ (MeV)	Tabakin potential (second order), experimental energies		$E$ (MeV)	Serber force (Ref. 25), Yukawa well, experimental energies	
		$p_{1/2}(s_{1/2})^{-1}$	$p_{3/2}(s_{1/2})^{-1}$		$p_{1/2}(s_{1/2})^{-1}$	$p_{3/2}(s_{1/2})^{-1}$		$p_{1/2}(s_{1/2})^{-1}$	$p_{3/2}(s_{1/2})^{-1}$
0	26.6	1.000	0.000	27.7	1.000	0.000	27.7	1.000	0.000
1	27.3	0.183	-0.983	25.9	0.183	-0.983	25.9	0.378	-0.926
1	31.5	0.983	0.183	29.6	0.983	0.183	29.6	0.926	0.378
2	22.9	0.000	1.000	24.5	0.000	1.000	24.5	0.000	1.000

TABLE XII. Squared matrix elements for muon capture to individual states for  ${}^4\text{He}$ .

$T=1$ $J$	$E$ (MeV)	Tabakin potential (second order), calculated energies			$E$ (MeV)	Tabakin potential (second order), experimental energies			$E$ (MeV)	Serber force (Ref. 25), Yukawa well, experimental energies		
		$(M_V^2)_D^{(i)}$	$(M_A^2)_D^{(i)}$	$(M_P^2)_D^{(i)}$		$(M_V^2)_D^{(i)}$	$(M_A^2)_D^{(i)}$	$(M_P^2)_D^{(i)}$		$(M_V^2)_D^{(i)}$	$(M_A^2)_D^{(i)}$	$(M_P^2)_D^{(i)}$
0	26.6		0.017	0.052	27.7		0.016	0.049	27.7		0.016	0.049
1	27.3	0.073	0.026		25.9	0.078	0.028		25.9	0.047	0.038	
1	31.5	0.064	0.020		29.6	0.070	0.022		29.6	0.096	0.013	
2	22.9		0.102	0.123	24.5		0.095	0.114	24.5		0.095	0.114

This table also includes our estimates for the ratio of the  $E1$  transition probability of the upper  $1^-, T=1$  state to the ground state with respect to that of the lower  $1^-, T=1$  state, with and without the energy weighting factor.

We now use our results on the spectrum to compute the dipole components of the squared matrix elements and the total capture rate for muon capture in the  $\alpha$  particle. We carry out this calculation for all of the potentials which we used in obtaining the  $T=1$  levels in Fig. 2. Since our levels are obviously split too much, we also perform a calculation using the experimental energies of the  $T=1$  states, as found in  ${}^4\text{Li}$ , in conjunction with the configuration mixing of the  $1^-, T=1$  states, as predicted by our second-order calculation with the Tabakin potential. For comparison we repeat the same

calculation using the configuration mixing determined in SW for a Serber force and a Yukawa well. Since our most consistent calculation for the spectrum of  ${}^4\text{He}$  was performed with the Tabakin potential in second order, we list only our muon-capture results for this particular spectrum and for the experimental energies. However, a comparison of our results for all potentials used in calculating spectra in this paper will be given in the discussion of results.

Table XI lists the energies and coefficients of the particle-hole states for  $J^-, T=1$ , used in our muon-capture calculation. Using Eq. (27) we compute the squared matrix elements for muon capture to individual states, which are given in Table XII. Table XIII lists the squared matrix elements for the total muon-capture rate plus the results of FW for comparison, while Table

TABLE XIII. Squared matrix elements for the total muon-capture rate for  ${}^4\text{He}$ . The primed results are those of Foldy and Walecka (Ref. 28).

Potential	$(M_V^2)_D$	$(M_A^2)_D$	$(M_P^2)_D$	$(M_V^2)_{UD}$	$(M_A^2)_{UD}$	$(M_P^2)_{UD}$	$(M_V^2)_{D'}$	$(M_V^2)_{UD'}$
Tabakin (2nd order), calculated energies	0.137	0.165	0.175	0.159	0.195	0.207	0.094	0.108
Tabakin (2nd order), <sup>a</sup> experimental energies	0.148	0.161	0.163	0.173	0.188	0.193	0.094	0.108
Serber force <sup>b</sup> (Ref. 25), experimental energies	0.143	0.162	0.163	0.167	0.191	0.193	0.094	0.108

<sup>a</sup>  $(M_V^2)_D : (M_A^2)_D : (M_P^2)_D = 1 : 1.09 : 1.10$ .<sup>b</sup>  $(M_V^2)_D : (M_A^2)_D : (M_P^2)_D = 1 : 1.13 : 1.14$ .TABLE XIV. Square of the elastic form factor uncorrected for center-of-mass motion and ratios of the retarded to unretarded squared matrix elements for  ${}^4\text{He}$ .

Potential	$(M_V^2)_D / (M_V^2)_{UD}$	$(M_A^2)_D / (M_A^2)_{UD}$	$(M_P^2)_D / (M_P^2)_{UD}$	$ F_{el}(v_{res}) ^2$
Tabakin (2nd order), calculated energies	0.862	0.846	0.845	0.858
Tabakin (2nd order), experimental energies	0.855	0.856	0.845	0.858
Serber force (Ref. 25), experimental energies	0.856	0.848	0.845	0.858

TABLE XV. Total muon capture rate in  ${}^4\text{He}$ .

Theory	$\Lambda_{\mu c}$ ( $\text{sec}^{-1}$ )
Tabakin (2nd order), calculated energies	278
Tabakin (2nd order), experimental energies	262
Serber force with Yukawa well (Ref. 25)	272
Calculation of Foldy and Walecka (Ref. 28)	249
Experiment	$\Lambda_{\mu c}$ ( $\text{sec}^{-1}$ )
Bloch (Ref. 44)	$375 \pm 46$
Bizzarri <i>et al.</i> (Ref. 47)	$333 \pm 75$

XIV compares the ratio of  $(M_I^2)_D$  to  $(M_I^2)_{UD}$  with the elastic form factor squared,  $|F_{el}(\nu_{res})|^2$ . Finally, in Table XV, we give the total muon capture rate determined by using the computed ratios of  $(M_P^2)_D$  and  $(M_A^2)_D$  to  $(M_V^2)_D$  in the equations of FW.

#### IV. DISCUSSION OF RESULTS AND CONCLUSIONS

The purpose of this paper was to determine what kind of results we could obtain for a particle-hole calculation of nuclear spectra using realistic nuclear forces. We find that our results agree fairly well with experiment, even though the  $p$ -state contributions are overestimated, and obtain several new results and predictions from the inclusion of the  $p$ -state interaction. There have been only a few other particle-hole calculations of spectra with realistic forces, and they also give encouraging results. Green *et al.* obtained good agreement with the spectrum of  ${}^{16}\text{O}$  for a RPA calculation with a singular hard-core potential, while the results of Kallio and Koltveit for the same nucleus were not as good, since they used a realistic potential that acted only in  $s$  states.

From Table VII and Figs. 1 and 2, we conclude that for making shell-model calculations with realistic nucleon-nucleon potentials, the separable Tabakin potential and the singular, hard-core potentials of BGT and

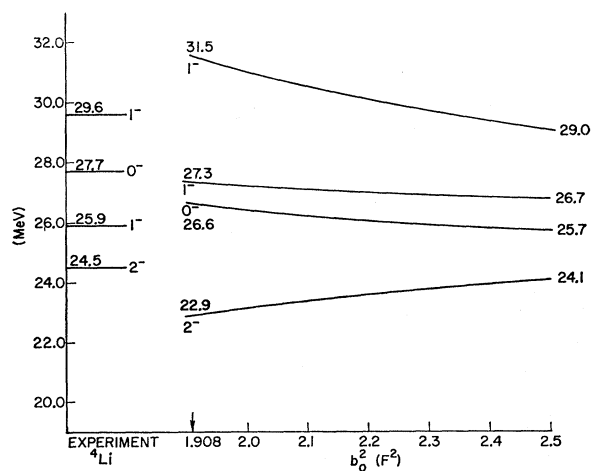


FIG. 6.  $T=1$  spectrum of  ${}^4\text{He}$ , determined from the Tabakin potential in second order, for increasing values of  $b_0^2$ . The arrow has the same meaning as in Fig. 3.

Hamada are *essentially equivalent potentials*.<sup>39</sup> In particular, the results for the Tabakin potential in second order and the averaged BGT potential are extremely similar. Consequently, in performing shell-model calculations we can choose whichever potential is most convenient for taking matrix elements. In our case we found that the Tabakin potential, being separable, greatly simplified calculations and also allowed us to treat the  $s$ -state interactions *consistently* with respect to the  $p$ -state and higher state interactions. As stated in the introduction, Kuo *et al.* performed a calculation of nuclear spectra with the Tabakin potential and also found that it is a convenient potential with which to make calculations and that it gives matrix elements consistent with those determined for a singular, hard-core potential.

Again from Figs. 1 and 2 we observe that the effect of the tensor force is quite large, particularly in the  $T=0$  states. Since  ${}^3I_1^{ls}$  and  ${}^3I_1^t$  have almost the same absolute magnitude and since  ${}^3I_1^q$  is quite small (Table VII), the difference in the  $T=0$  splittings from the spin-orbit form, as predicted by the Landé interval rule in SW, is caused by the large angular-momentum coupling factors which multiply the tensor term for  $\mathcal{J}=0$  and 1 [see Eqs. (42) and (44)].

From our calculation we obtain the significant prediction for the  $J^-, T=0$  states that the  $0^-$  state lies close to the  $2^-$  state and that the  $1^-$  state lies far above the  $0^-$  and  $2^-$  states. We are encouraged that our calculation of the ordering of the above states is basically correct by the fact that a  $0^-, T=0$  state in the close neighborhood of the  $2^-, T=0$  state is consistent with the experimental observations of Meyerhof<sup>40</sup> on the excited states of the  $\alpha$  particle. In fact, such a state will probably explain what earlier appeared to be an inconsistency in the experimental results regarding the ratio of the expansion coefficients  $B_2$  and  $B_0$ . We would encourage any interested experimentalists to look for the  $0^-$  and  $1^-, T=0$  states of  ${}^4\text{He}$ , particularly the  $0^-$  state.

Since we have performed only a one-particle-one-hole calculation, it is impossible for us to make any predictions about the observed  $0^+, T=0$  state. Szydlik<sup>41</sup> has carried out a two-particle-two-hole calculation with a Serber force and obtains a  $0^+, T=0$  state as the lowest excited state of the  $\alpha$  particle.

Our results for the  $J^-, T=1$  states need to be improved, since the splittings among the levels are too large and since the  $0^-$  and the lower  $1^-$  states are inverted in three of our four calculations and are barely

<sup>39</sup> Since we have calculated the spectrum with three entirely different potentials fit to the same experimental data, the above result indicates that the calculated spectrum would not change appreciably for variations of the potential parameters allowed by the experimental limits on the observed scattering data.

<sup>40</sup> W. E. Meyerhof, Bull. Am. Phys. Soc. **10**, 698 (1965). Also B. R. Barrett, W. E. Meyerhof, and J. D. Walecka, Phys. Letters **22**, 450 (1966); and C. Werntz and W. E. Meyerhof, Bull. Am. Phys. Soc. **12**, 12 (1967).

<sup>41</sup> P. P. Szydlik and R. J. Philpott, Bull. Am. Phys. Soc. **12**, 47 (1967).

in the correct order in the fourth. From Figs. 5 and 6 we see that increasing  $b_0$ , i.e., decreasing the overlap of the wave functions in the matrix elements, does not change the ordering of any of the levels. So in this respect our calculation is independent of  $b_0$ . At first this result might appear to be quite surprising, since as  $b_0$  increases, the  $p$ -state matrix elements approach zero faster than the  $s$ -matrix elements, and our results should approach those in SW. However, this statement is incorrect, since SW empirically included the spin-orbit splitting as a constant in their calculation. But the spin-orbit splitting comes only from the triplet  $p$  interaction and, thus, decreases with increasing  $b_0$ . We note that if we include a constant splitting between the  $0^-$  and  $2^-$ ,  $T=1$  states that the lower  $1^-$  and  $0^-$ ,  $T=1$  states will cross for increasing  $b_0$ .

We also note that the calculated splitting for the two  $2^-$  states is never more than 0.7 MeV, which is much smaller than the experimental splitting. This result follows from the fact that the quantity  ${}^1I_0(0) - {}^1I_1(1) - {}^3I_0(1)$  in Eq. (18) is small and remains *essentially constant* for increasing  $b_0$ . Thus, it is apparent from both of the above results that our calculation must be improved by more than increasing  $b_0$  in order to get the correct spectrum.

Returning to Eqs. (12), (18), (20), (42), and (44), we observe that we can express our seven theoretical equations [i.e., six equations for the energy splittings and one equation for  $V_{1/2\ 3/2}(1-1)$ , which causes the configuration mixing of the two  $1^-$ ,  $T=1$  states] in terms of *only four quantities*,  ${}^3I_1^t$ ,  ${}^3I_1^{1s}$ ,  $-{}^3I_0(1) + {}^1I_1(1)$ , and  $-{}^3I_1^c + {}^1I_1(1)$ . Consequently, we are able to obtain two important results.

First, we can eliminate these four quantities from our seven equations to obtain three relationships which depend *only upon the experimental energy splittings*.<sup>40</sup> In particular we obtain two relationships which give the two experimentally unobserved splittings [ $E(2^-) - E(0^-)$  and  $E(1^-) - E(0^-)$ ] in terms of observed splittings. Substituting in the experimental splittings, we find that

$$E(2^-) - E(0^-) = 0.0 \pm 0.5 \text{ MeV}, \quad (48)$$

and

$$E(1^-) - E(0^-) = 6.4 \pm 1.2 \text{ MeV}, \quad (49)$$

where we have arbitrarily assigned an error of  $\pm 250$  keV to the experimental splittings to get an idea of the sensitivity of our answers. Equation (48) is in excellent agreement with the prediction of Meyerhof from the experimental data that the  $0^-$ ,  $T=0$  state in  ${}^4\text{He}$  lies within  $\frac{1}{2}$  MeV of the  $2^-$ ,  $T=0$  state.

The third equation gives  $V_{1/2\ 3/2}(1-1)$  which in turn gives the ratio of the  $E1$  transition probabilities in terms of the observed splittings. Again substituting in the experimental splittings, we obtain

$$(\Delta E_+ / \Delta E_-)^3 | \langle 1P_1 | \Psi_+ \rangle |^2 / | \langle 1P_1 | \Psi_- \rangle |^2 = 0.43 \pm 0.09. \quad (50)$$

Hence, our theory, *independent of the radial dependence of the potential*, plus the four observed energy splittings for nuclei with  $A=4$  makes three predictions, of which two are in excellent agreement with experiment. The third result cannot be checked, since the splitting between the  $1^-$  and  $0^-$ ,  $T=0$  states has not yet been observed.

Secondly, we can use the four observed splittings to determine the four quantities  ${}^3I_1^t$ ,  ${}^3I_1^{1s}$ ,  $-{}^3I_0(1) + {}^1I_1(1)$ , and  $-{}^3I_1^c + {}^1I_1(1)$  and, thereby, obtain some idea of how and where we need to improve our calculation of the two-body matrix elements in order to achieve agreement with experiment. Using the experimental splittings, we find that

$$\begin{aligned} {}^3I_1^t &= 0.9 \text{ MeV}, & {}^3I_1^{1s} &= -1.1 \text{ MeV}, \\ -{}^3I_0(1) + {}^1I_0(0) &= 2.1 \text{ MeV}, \\ \text{and} \\ -{}^3I_1^c + {}^1I_1(1) &= -1.2 \text{ MeV}, \end{aligned} \quad (51)$$

which are reasonable results, except for the last one, since  ${}^1V_{-c}$  is fairly strong and repulsive and  ${}^3V_{-c}$  is weak and attractive.

But we know from experiment that all the observed levels have widths of  $\frac{1}{2}$  MeV or more. Hence, let us try to determine four reasonable values of the above quantities *which fit all the levels of the observed spectrum within a few tenths of a MeV*. Doing this, we obtain

$$\begin{aligned} {}^3I_1^t &= 0.8 \text{ MeV}, & {}^3I_1^{1s} &= -1.1 \text{ MeV}, \\ -{}^3I_0(1) + {}^1I_0(0) &= 3.1 \text{ MeV}, \\ \text{and} \\ -{}^3I_1^c + {}^1I_1(1) &= 0.8 \text{ MeV}. \end{aligned} \quad (52)$$

The results of Eq. (52) still predict that the  $0^-$ ,  $T=0$  state lies within  $\frac{1}{2}$  MeV of the  $2^-$ ,  $T=0$  state. They also predict a small value of  $V_{1/2\ 3/2}(1-1)$ , so that the energy weighted ratio of the  $E1$  transition probabilities is 1.07. Thus, reasonable values of the  $I$ 's can be found which reproduce the experimental data.

We note that the results of Eq. (52) are exactly what we would expect from a more accurate calculation, i.e., a decrease in the  $p$ -state contributions with little change in the  $s$ -state contributions. We already know that our  $p$ -state matrix elements are too big and that their contributions are very sensitive to changes in the method of calculation, as our results for  ${}^3I_1^t$  and  ${}^3I_1^{1s}$  in Table VII for the underestimated and overestimated values clearly show. For the Tabakin potential we found that the second-order corrections to the potential were often quite large, particularly for the triplet  $s$  and singlet  $p$  interactions. Kerman *et al.* also found that second-order corrections were needed and improved their H-F calculation for the Tabakin potential. Consequently, we would expect higher order corrections to these matrix elements to be important. It is possible that  ${}^1I_1(1)$  may be greatly reduced in a higher order calculation, if the exact wave function is pushed out far enough, so

that it has only a small overlap with the repulsive singlet  $p$  potential.

If the splittings among the  $T=0$  states were really 12 to 14 MeV, as we calculate them to be, then some doubt would be cast upon the basic assumption of the supermultiplet theory. But, we know that these splittings will decrease for a more accurate calculation, since the  $p$ -state contributions will decrease, as we found in our calculation for increasing  $b_0$  and decreasing overlap. For example, from Figs. 5 and 6 we find that the  $T=0$  states are split by about 9 MeV, when the  $T=1$  levels are of the same order of magnitude as the experimental  $T=1$  levels in  ${}^4\text{Li}$ . Also our empirical results in Eq. (52) imply that the over-all splitting for the  $T=0$  states is only 6 MeV. Thus, it appears that the supermultiplet theory is theoretically valid for the  $\alpha$  particle.

*One of the most important results of our present calculation is that the spin-orbit splitting of the shell model can be explained in first order in terms of the relative two-body spin-orbit force.* The agreement between the experimental value<sup>42</sup> of  $\epsilon_{p_{1/2}} - \epsilon_{p_{3/2}}$  and our calculated values for the Tabakin potential and for the average values of the BGT and Hamada potentials is rather good, considering the fact that the calculated value depends only on the spin-orbit force multiplied by a large factor and that the spin-orbit force has the shortest range of all the components of the nuclear force and is, thus, the hardest force to determine from the experimental data. Our results for the  $p_{1/2} - p_{3/2}$  spin-orbit splitting are consistent with the H-F calculation of Kerman *et al.* for  ${}^{16}\text{O}$  and  ${}^{40}\text{Ca}$ . In both of their calculations they obtained spin-orbit splittings that are larger than the experimental splittings. Since they were unable to separate the effect of their potential into components, as we did in Eq. (42), they suggested that significant differences in the  $p_{1/2}$  and  $p_{3/2}$  wave functions indicated that the tensor force was causing the spin-orbit splitting to be too large. However, any tensor-force contributions must be in second order, since only the relative spin-orbit interaction contributes to the  $p_{1/2} - p_{3/2}$  spin-orbit splitting in first order. Since the spin-orbit force occurs only in relative  $p$  states for  ${}^4\text{He}$  and since SW used a Serber force in their calculation, they found no splitting between the  $p_{1/2}$  and  $p_{3/2}$  S-P levels.

The calculated values of the center of gravity of the supermultiplet agree with the experimental values to  $\frac{2}{3}$  MeV out of 26 MeV, and the agreement becomes even better for increasing  $b_0$ .

While the ratios of the  $E1$  transition probabilities determined for the BGT and Hamada potentials are of the same order as those found by SW, those obtained for the Tabakin potential are much smaller and are in closer agreement with the observed ratio, which is  $\sim \frac{1}{2}$ . These smaller ratios come from the fact that the off-diagonal matrix element calculated for the Tabakin potential is smaller than the one calculated for the hard-

core potentials. The energy weighted ratios are, of course, larger. However, the experimental ratio is probably somewhat larger than  $\frac{1}{2}$ , because of uncertainties in the widths of the levels.<sup>40</sup>

Our calculation for muon capture in  ${}^4\text{He}$  shows that the results determined using a potential without a tensor force, as in SW, are not much different from those determined using a tensor force.

From the  $1^-$ ,  $T=1$  states calculated in SW,

$$(M_V^2)_D = (M_A^2)_D = (M_P^2)_D, \quad \text{to within 14\%};$$

and

$$(M_I^2)_D / (M_I^2)_{UD} = |F_{e1}|^2, \quad \text{to within 1.5\%}.$$

For the Tabakin potential in second order, which included the tensor interaction, we found that

$$(M_V^2)_D = (M_A^2)_D = (M_P^2)_D, \quad \text{to within 10\%};$$

and

$$(M_I^2)_D / (M_I^2)_{UD} = |F_{e1}|^2, \quad \text{to within 1.5\%};$$

when we assumed capture to the experimental energy levels but used the configuration mixing predicted by our calculation.

When we assumed capture to the calculated energy levels, we found that the squared matrix elements were equal to only 28%, while the ratio of the retarded to the unretarded matrix elements remained equal to  $|F_{e1}|^2$  to within 1.5%. For similar calculations with the hard-core potentials for capture to the calculated energies, we again found that the squared matrix elements were equal to about 30% and that the retarded-unretarded ratio was equal to  $|F_{e1}|^2$  to about 2.0%.

It is not surprising that the results for capture to the calculated levels are so poor, since the levels are split too far apart. The calculation for capture to the experimental levels using the calculated configuration mixing makes sense, since we have already shown that it is possible to decrease the splittings without appreciably changing the configuration mixing. The equality of the squared matrix elements to within 10% for a shell-model calculation is consistent with the results of similar calculations for other nuclei.<sup>32</sup> Since the supermultiplet theory predicts that  $M_A^2 = M_V^2 = M_P^2$  for spin-independent forces, the fact that they are still equal to within 10% for spin-dependent forces again indicates that the supermultiplet theory is theoretically valid for the  $T=1$  states in  ${}^4\text{He}$ .<sup>43</sup>

In all of our calculations we found that  $(M_V^2)_{UD}$  was about twice the value obtained by FW. This result is again consistent with the muon-capture calculations of de Forest in other nuclei. Since  $(M_I^2)_D / (M_I^2)_{UD} = |F_{e1}|^2$  to within 1.5%, we conclude that this assumption by FW is also correct for  ${}^4\text{He}$ .

<sup>43</sup> If we use the *empirically* determined configuration mixing discussed earlier (also Ref. 40), we find that the agreement is much better with  $M_V^2 = M_A^2 = M_P^2$  to within 5%. This result is true for any nucleon-nucleon force which gives rise to the observed splittings within the [15] supermultiplet in  ${}^4\text{He}$ .

<sup>42</sup> P. Fessenden and D. R. Maxson, Phys. Rev. **133**, B71 (1964).

The total muon-capture rates are found to be slightly larger than the one found by FW. If we include the effect of the  $d$ -state admixture, which is  $(38 \pm 20) \text{ sec}^{-1}$ ,<sup>44</sup> and take the maximum admixture and the minimum capture rate predicted by experiment,<sup>45,46</sup> then the calculated and experimental capture rates are approximately equal. But the agreement is obviously not good, since we are taking the extreme limits in our favor. The total capture rates are larger for the hard-core potentials, since the matrix elements are equal to only 30% in these cases. One cannot have agreement on both of the above results. If the squared matrix elements are almost equal, then the total capture is about the same as that found by FW and, hence, too small. On the other hand, if the matrix elements are not equal by a large percent, then the total capture rate is considerably larger.

In general, our results agree fairly well with experiment, which is somewhat surprising, since we have performed our calculations with harmonic-oscillator wave functions for bound states, when we really should have used plane wave functions. Not only have we performed a first-order calculation in this manner but also a second-order calculation for the Tabakin potential. How can we justify such a calculation and why should our results be as good as they are?

The answer to these questions appears to come from the fact that the first excited states of  ${}^4\text{He}$  are  $p$  states. Hence, there is an angular-momentum barrier, given by  $\hbar^2 l(l+1)/2Mr^2$ .<sup>47</sup> For  $l=1$  and  $r$  equal to the root-mean-squared radius of the  $\alpha$  particle, i.e.,  $r_{\text{rms}}({}^4\text{He}) = 1.46 \text{ F}$ ,<sup>28</sup> we find that the angular-momentum barrier has a height of 19.5 MeV above the zero of the potential. But from the neutron and proton separation energies for  ${}^4\text{He}$ , we know that the ground state is about 20 MeV below the zero of the potential. Therefore, nucleons in excited states at 20 to 30 MeV above the ground state are held in by the angular-momentum barrier, causing

them to make several reflections inside the effective potential well before escaping. Because of this barrier, the approximation of the excited-state wave functions by bound-state wave functions is greatly strengthened.

We also note that Tabakin<sup>10</sup> has done a second-order calculation with his separable potential in nuclear matter, i.e., for plane-wave states, and that his second-order corrections, percentagewise, are of the same order as ours obtained for harmonic-oscillator wave functions in  ${}^4\text{He}$ . Thus, it would appear that we have not introduced any large errors in our calculation by using harmonic-oscillator wave functions instead of plane-wave virtual states.

To summarize we find that a particle-hole calculation of the spectrum of the  $\alpha$  particle with realistic nuclear forces gives fairly good agreement with experiment, especially for a *no-adjustable-parameter* calculation, and allows us to draw three new and significant conclusions, which SW were not able to obtain, since they used a Serber force:

1. The spin-orbit splitting of the S-P shell-model states  $p_{1/2}$  and  $p_{3/2}$  is caused in first order only by the relative two-body spin-orbit interaction in  $p$  states.
2. The  $0^-, T=0$  state is depressed by the strong tensor force and is found to lie close to the  $2^-, T=0$  state. This predicted  $0^-, T=0$  state is consistent with present experimental data.
3. The squared matrix elements for muon capture are equal to within 10%, implying that the supermultiplet theory is valid for the  $T=1$  states of the  $\alpha$  particle. We also find that  $(M_I^2)_D/(M_I^2)_{UD} = |F_{01}|^2$  to within 1.5%. The total muon capture rate in  ${}^4\text{He}$  is still found to be too small.

#### ACKNOWLEDGMENTS

The author wishes to thank Professor J. D. Walecka for suggesting this problem and for many helpful and stimulating discussions while work was in progress. The author is also grateful to Professor W. E. Meyerhof for discussions regarding his experimental results on the excited states of the  $\alpha$  particle and to D. J. Silverman for his assistance in setting up the computer programs for calculating the matrix elements.

<sup>44</sup> C. A. Caine and P. S. H. Jones, Nucl. Phys. **44**, 177 (1963).

<sup>45</sup> M. Bloch [private communication to Foldy and Walecka, Ref. (28)].

<sup>46</sup> R. Bizzarri, E. D. Capua, U. Dore, G. Gialanella, P. Guidoni, and I. Laakso, Nuovo Cimento **33**, 1497 (1964).

<sup>47</sup> We thank Professor R. J. Oakes for a valuable discussion on this point. Also R. J. Oakes and C. N. Yang, Phys. Rev. Letters **11**, 174 (1963).